[American Journal of Science, Vol. 304, January, 2004, P. 67–101]

CHROMIUM GEOCHEMISTRY IN SERPENTINIZED ULTRAMAFIC ROCKS AND SERPENTINE SOILS FROM THE FRANCISCAN COMPLEX OF CALIFORNIA

CHRISTOPHER OZE*†, SCOTT FENDORF, DENNIS K. BIRD, and ROBERT G. COLEMAN

Department of Geological and Environmental Sciences, Stanford University, Stanford, California 94305-2115, USA

ABSTRACT. Weathering of ultramafic rocks and serpentinites in the Franciscan Complex of California produces serpentine soils containing high concentrations of Cr as well as other potentially toxic elements including Ni, Co, and Mn. Chromium concentrations in serpentine soils from Jasper Ridge Biological Preserve in the Central Coast Range are as high as 4,760 mg kg^{-1}, nearly three times greater than the serpentinite protolith (~1800 mg kg^{-1}). Chromium-containing minerals within the bedrock include chlorite (~0.3 Cr wt. %), enstatite (~0.4 Cr wt. %), augite (~0.7 Cr wt. %), chromite (~10.8 Cr wt. %), magnetite (8.2-10.3 Cr wt. %), and an ultra fine-grained mixture of spinel and a silicate phase containing ~13.3 Cr weight percent. Chromium concentrations in serpentine soil profiles fluctuate between 1,725 to 4,760 mg kg^{-1} and do not correspond to variations in soil pH, organic carbon, or electrical conductivity. The enrichment and variability of soil Cr is directly related to the modal abundance and weathering of chromite, Cr-magnetite, and the spinel-silicate mixture. By comparison, Cr silicates account for < 10 percent of the total soil Cr. Chemical analyses and X-ray microprobe maps demonstrate that Cr-spinels in these soils undergo incongruent dissolution progressively enriching the spinel toward a Cr-enriched end-member ($FeCr_2O_4$). Chromium occurs in the trivalent state in both the rock and soil samples. The apparent resistance of Cr-spinels to weathering, evident from extraction experiments, suggests that these minerals are not large inputs for Cr in soil solutions and vegetation associated with serpentine soils. Chromium-bearing igneous and metamorphic silicates in the protolith and Cr-bearing clay minerals in the soil are more likely sources of chemically mobile and bioavailable Cr.

INTRODUCTION

Serpentine soils are formed from the weathering of ultramafic rocks and their metamorphic equivalents (serpentinites; Brooks, 1987). Measured Cr concentrations in these soils range as high as 80,600 mg kg^{-1} and are enriched compared to non-serpentine soils (7 to 221 mg kg^{-1}; McBride, 1994; Proctor, 1992). The distribution and concentration of Cr in serpentine soils worldwide is highly variable due to the chemical composition and mineralogy of the parent material and soil forming factors including climate, biota, topography, precipitation, and time (Hotz, 1964; Rabenhorst and others, 1982; Schwertmann and Latham, 1986; Brooks, 1987; Schreier and others, 1987; Alexander and others, 1989; Gough and others, 1989; Kaupenjohann and Wilcke, 1995). Potential Cr-bearing phases in serpentine soils have been assessed using extraction experiments and these phases include organic material, silicates, secondary oxides, and spinels (Schwertmann and Latham, 1986; Alexander and others, 1989; Gasser and Dahlgren, 1994; Kaupenjohann and Wilcke, 1995; Becquer and others, 2003). The weathering of these Cr-bearing phases over geologic time and how these sources govern the distribution of Cr in serpentine soils have not been evaluated in great detail.

*Current Address: Department of Earth Sciences, Dartmouth College, 6105 Fairchild Hall, Hanover, New Hampshire 03755; oze@dartmouth.edu
†Corresponding author

Chromium is a group VIB transition metal present in the environment as Cr(III), a non-hazardous species and micronutrient, and/or as Cr(VI), a toxin to living cells and a Class A human carcinogen by inhalation (Daugherty, 1992; Cohen and others, 1993; James and others, 1997). Chromium(III) is chemically immobile due to forming low solubility (oxy)hydroxides and stable surface complexes, whereas, Cr(VI) is a weakly adsorbing (oxy)anion and thus is mobile in most aquatic environments (McBride, 1994; Fendorf, 1995; Ball and Nordstrom, 1998). Chromite and Cr-magnetite have been cited as primary sources of Cr in serpentine soils (Rabenhorst and others, 1982; Schwertmann and Latham, 1986; Alexander and others, 1989; Gough and others, 1989). Although Cr is primarily found in the form of Cr(III) in both ultramafic rocks and serpentinites, Cr(VI) has been measured in serpentine soils in California and New Caledonia (Gough and others, 1989; Becquer and others, 2003). Due to the abundance of Cr and the possible formation of Cr(VI), serpentine soils and serpentinites are potential sources of non-anthropogenic Cr contamination.

The objectives of this study are to determine the distribution and chemistry of Cr in naturally Cr-enriched soils using an integrated field, analytical, experimental, and theoretical approach. A wide array of techniques and methods including X-ray absorption spectroscopy and chemical extractions were used to identify the nature of Cr and its availability in serpentine soils. Serpentinites and serpentine soils at Jasper Ridge Biological Preserve located near Stanford, California, were used to evaluate the geochemical behavior of Cr. These soils cover approximately 50,000 m^2 and contain high concentrations of the trace elements Cr, Ni, and Mn. The soils are dominantly Mollisols with grassland vegetation and they are pedagogically similar to those associated with the Central Coast Range of the Franciscan Complex in the western United States. The main serpentinite body at Jasper Ridge was exposed approximately 400,000 years ago allowing pedogenesis and Cr cycling to occur over a geologically relevant time period (Burgmann and others, 1994). These soils can then be used as a proxy for evaluating the long-term behavior of Cr.

BACKGROUND

Geologic Background of the Serpentinite at Jasper Ridge

Jasper Ridge Biological Preserve is located in the foothills of the Santa Cruz Mountains in California and is part of the Central Coast Range of the Franciscan Complex, an Early Cretaceous accretionary mélange containing blocks of graywacke, greenstone, blueschist, and serpentinized ophiolite (fig. 1). Formation, metamorphism, and emplacement of serpentinite at Jasper Ridge began approximately 130 to 150 million years ago during Jurassic subduction along the California continental margin (Page and Tabor, 1967). Thin wedges of ultramafic rock (peridotite) were detached from the down-going slab of oceanic crust and incorporated into the subduction mélange. Subsequent serpentinization of the ultramafic rock in the down-going slab resulted in the formation of serpentinites now exposed at Jasper Ridge.

Rare blueschist blocks (1-5 meters in width) present in the serpentinite at Jasper Ridge attest to the degree of metamorphism and the depths from which portions of the tectonic mélange has been elevated. Transformation of greenstone in the mélange into blueschist required high pressures in excess of ~5 to 7 kbars (15 - 20 km depth) and temperatures of 200° to 300°C (Ernst, 1971). The low density of the serpentine (2.45 - 2.50 g cm^{-3}) allowed upward diapiric migration of the serpentinite body through the denser enclosing tectonic mélange (2.65 g cm^{-3}). Uplift of the present day Coast Range and activity associated with the San Andreas fault system have shaped the current topography and exposure of serpentinite at Jasper Ridge. Serpentinite is currently present as a narrow discontinuous band of pervasively sheared rock located

along the ridge top (fig. 1). The serpentinite is in fault contact with the Whiskey Hill Formation (Cretaceous turbidic sandstone and mudstone) and tectonically interleaved with the Franciscan Complex.

Serpentine Soil: Characteristics

Relative to other soil types, serpentine soils are characterized by elevated concentrations of Cr, Ni, Co, and Fe, lower concentrations of plant nutrients such as Ca, K, N, and P, lower Ca/Mg ratios, and characteristic flora and physical properties (Brooks, 1987). The pH of serpentine soils ranges from ~4 up to 9 (Brooks, 1987; Cole, 1992; Proctor, 1992). Serpentine soil solutions obtained using tension-free lysimetry have Cr concentrations between 0.1 and 3.2 μmol L^{-1}, in which a majority of the Cr is present as colloidal material (Gasser and Dahlgren, 1994). The inhabitability of these soils for most plants has been attributed to the imbalance of Ca to Mg (Walker, 1954), the deficiency of plant nutrients (Turitzin, 1991), and the elevated concentration of heavy metals (Robinson and others, 1935); however, linking the lack of plant productivity of these soils to toxic levels of Cr has not been fully resolved (Brooks, 1987; Kruckeberg, 1992). The unique flora and fauna associated with these soils have been well-documented and Cr concentrations in the plants range as high as 600 mg kg^{-1} (Brooks, 1987; Gough and others, 1989).

Chromium concentrations as a function of depth for serpentine soils in Maryland (Rabenhorst and others, 1982), Tehama County, California (Gough and others, 1989), the Klamath Mountains, California (Hotz, 1964), and Newfoundland, Canada (Roberts, 1992), are illustrated in figure 2. Chromium concentrations with respect to depth at each location are highly variable demonstrating both maximums and minimums. The concentration of Cr varies significantly at each location due to the chemical composition of the parent material and other soil-forming factors; nevertheless, Cr concentrations typically decrease with depth towards the bedrock.

A variety of chemical extractions on serpentine soils suggest a broad host of Cr-containing soil phases including organic material, silicates, secondary oxides, and spinels (Schwertmann and Latham, 1986; Alexander and others, 1989; Gasser and Dahlgren, 1994; Kaupenjohann and Wilcke, 1995). The maximum concentration of Cr extracted from a serpentine soil reported in the literature is 2.26 percent of the total Cr from the New Caledonia laterite using a 0.3 M dithionite-citrate bicarbonate (DCB) solution (Schwertmann and Latham, 1986). Li and Fendorf (2000) performed extractions on the serpentine soils at Jasper Ridge using organic acids (citric and oxalic acids) in which a 100 μM citric acid solution was only able to remove 23 Cr $\mu g\ g^{-1}$ (0.8 % Cr) from a soil containing ~3,000 Cr mg kg^{-1}. The small amount of Cr released suggests a majority of Cr is bound in phases that are not reactive with these solvents.

Sources of Chromium: Protolith/Bedrock

Chromium primarily occurs within oxide and silicate phases in ultramafic rocks and serpentinites. Chromite is a common primary (igneous) Cr-bearing spinel in mafic and ultramafic rocks and often survives low-grade metamorphic processes related to serpentinization (Hoffman and Walker, 1978; Malpas, 1992). Isomorphic substitution of Al^{3+}, Fe^{3+}, and Ti^{4+} into the octahedral site, and Mg^{2+}, Ni^{2+}, Zn^{2+} and Mn^{2+} into the tetrahedral site is common (Sack and Ghiorso, 1991); however, end-member chromite ($FeCr_2O_4$) is atypical (Cooper, 1980; Raase and others, 1983; Von Knorring and others, 1986; Treloar, 1987; Pan and Fleet, 1991; Burkhard, 1993; Christofides and others, 1994; Challis and others, 1995; Sanchez-Vizcaino and others, 1995; Deer and others, 1996; Mathiesen, ms, 1999). Pyroxenes such as augite ($\leq$ 1 Cr wt. %) and enstatite ($\leq$ 10 Cr wt. %) are primary minerals in ultramafic rocks that incorporate varying concentrations of Cr into their structures (Deer and others, 1996).

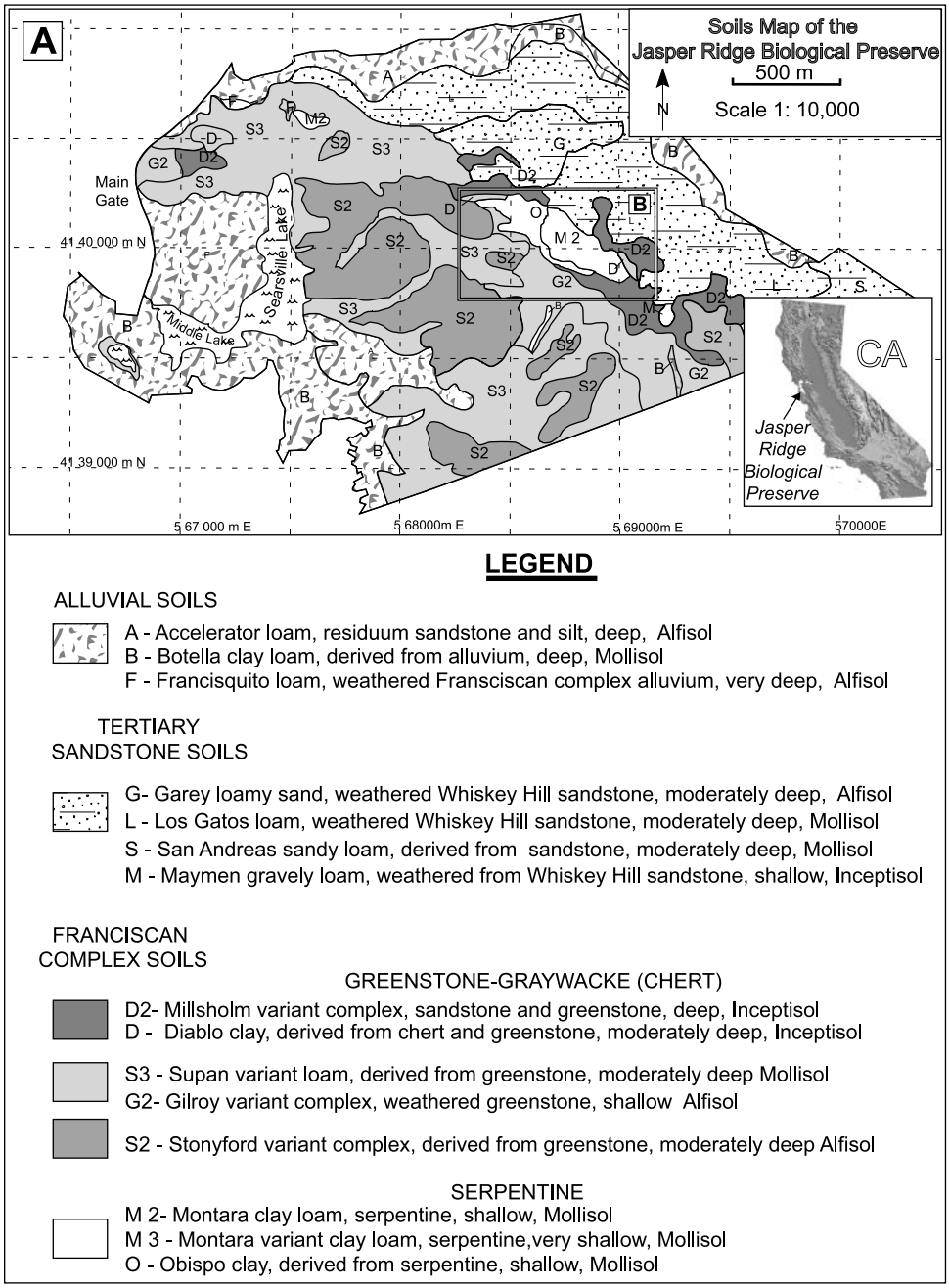

Fig. 1. (1A) Soils map of Jasper Ridge Biological Preserve (Stanford, CA) with descriptions of the soils shown in the legend.

Serpentinization is associated with the partial oxidation of Fe(II) present in olivine and pyroxene and its incorporation into magnetite (Brooks, 1987). Chromium(III) derived from primary chromite and pyroxene may isomorphically substitute into the Fe(III) site of magnetite due to size (octahedral radii: Cr^{3+} = 0.615 Å and

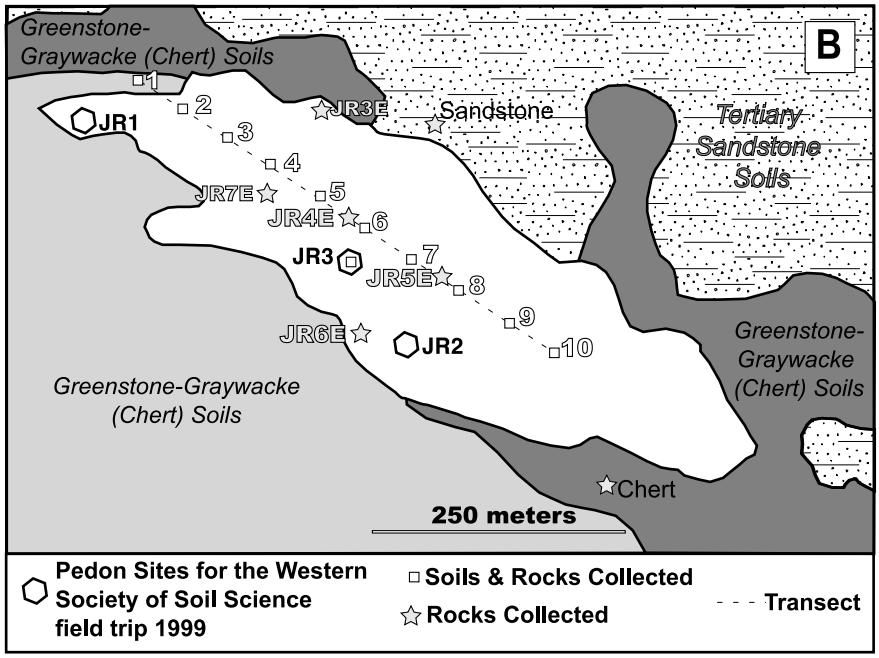

Fig. 1. (1B) An enlarged image of the study area shown in 1A indicating sampling sites of the soils and rocks collected. A dashed line marks the 500-meter transect.

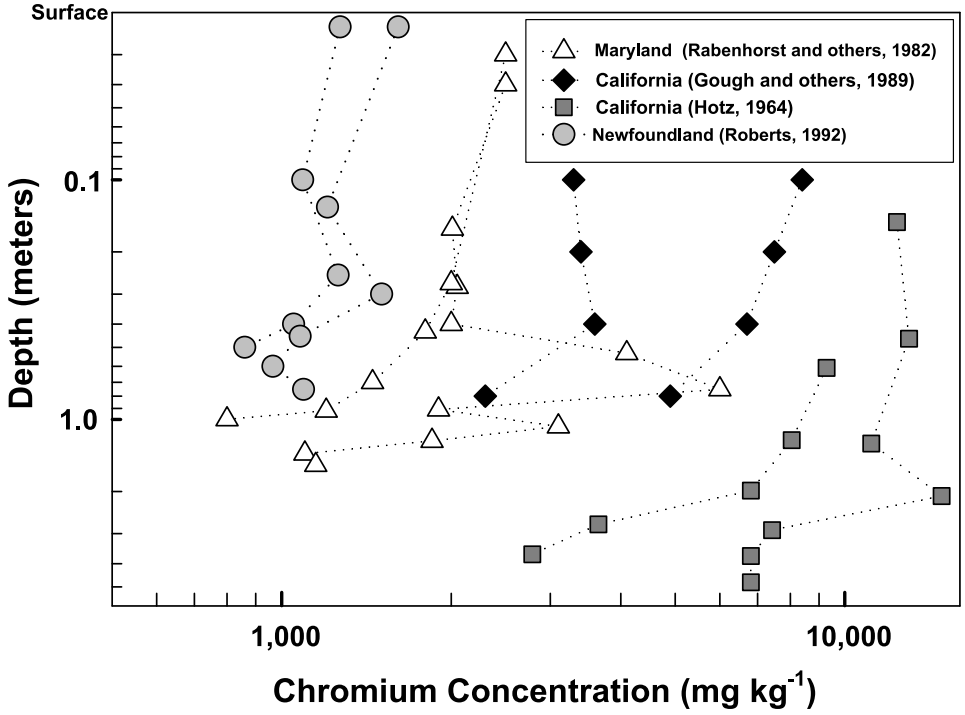

Fig. 2. Chromium concentrations (mg kg^{-1}) as a function of depth (m) for selected serpentine soils indicated in the key above.

Fe^{3+} = 0.643 Å) and charge similarities. Hydrothermal and CO_2 metasomatism of ultramafic rocks may produce Cr-silicate minerals including "fuchsite/mariposite" (Cr-mica: < 17 Cr wt. %), "uvarovite" (Cr-garnet: < 20 Cr wt. %), "tawmawite" (Cr-epidote: < 10 Cr wt. %), and "kämmererite" (Cr-chlorite: < 6 Cr wt. %); (Whitmore and others, 1946; Leo and others, 1965; Chen and Lee, 1974; Phillips and others, 1980; Schreyer and others, 1981; Max and others, 1983; Treloar, 1987; Kerrich and others, 1987; Pan and Fleet, 1991; Christofides and others, 1994; Sanchez-Vizcaino and others, 1995). These minerals, common in altered ultramafic rocks, have varying concentrations of Cr that isomorphically substitute for octahedral Al in the silicate structure due to similarities in charge, octahedral preference, and octahedral radii (Al^{3+} = 0.61 Å). Any of these silicates and magnetite are potential sources for Cr in soils produced by the weathering of serpentinite and ultramafic rocks.

Chromium-bearing Phases in Soils

Soil minerals, specifically Fe(III) (oxy)hydroxides and clays, provide a host of structural and surface sites that may sequester Cr(III) released to soil solution by weathering of Cr-bearing phases in serpentinite and ultramafic rocks. Isomorphic substitution of Cr(III) for Fe(III) in oxides, (oxy)hydroxides, and amorphous compounds is expected based on crystallographic considerations, synthesis experiments, and analyses of selective dissolution of Fe(III) phases (Schwertmann and others, 1989; Gerth, 1990). Additionally, Cr(III) readily sorbs on surfaces of Fe(III)-containing oxides such as magnetite and hematite via inner-sphere complexation and forms low-solubility precipitates at pH values greater than 4 (Charlet and Manceau, 1992; Peterson, 1996). Octahedral substitution of Cr(III) for Al(III) in clays (smectites and vermiculites) is possible based on size and charge similarities. Sorption of Cr(III) on edge and interlayer sites of clay minerals has also been observed by Ilton and Veblen (1994) and Ilton and others (2000). Soil organic matter (SOM) is another possible host for soil Cr in which Cr can be chelated into stable organomineral and organometallic complexes (Kaupenjohann and Wilcke, 1995; Brady and Weil, 1999).

MATERIALS AND METHODS

Location and Sample Collection

Jasper Ridge Biological Preserve is a microcosm of accreted terranes located in the foothills of the Santa Cruz Mountains, California. Figure 1A is a soils map reported by Kashiwagi (1985) depicting the alluvial, Tertiary sandstone, and Franciscan Complex soils present at Jasper Ridge. The Franciscan Complex soils are divided into two subgroups, those derived from greenstone-graywacke and those from serpentinite. The serpentine soils, dominantly Mollisols, and serpentinite bedrock are present as a narrow discontinuous band located along the ridge top, they do not receive sediment from the adjacent non-serpentine soils. Soils and rocks were collected at Jasper Ridge from 1999 to 2002 and sample locations are shown in figure 1B. A 500 meter transect consisting of 10 sites extends across the length of the serpentine soil body. At each site along the transect, soils and bedrock were collected with respect to depth using a soil corer. Site 1 (Diablo clay) is not derived from serpentinite, but rather from chert and greenstone. Additionally, Site 1 is located down slope of the main serpentinite body and has likely received sediment from the adjacent serpentine soil. Rocks were also collected at several exposed outcrops located in the serpentinite body.

Site JR3 (fig. 1B) was arbitrarily chosen for a detailed geochemical study to identify factors affecting the geochemistry of Cr in serpentine soils. Soil at JR3 is a

loamy, magnesic, thermic Lithic Haploxeroll. The thickness of the soil is approximately 50 centimeters deep. Grass, dominantly *Lolium multiflorum*, comprises 95 percent of the vegetation at this site and trees and shrubs are not present.

Mineral Identification in Rocks and Soils

Mineral identification was accomplished by electron probe microanalysis on an automated JEOL 733A electron microprobe operated at 15 kV accelerating potential and 15 nA beam current. Calibration was conducted using natural geologic standards. The beam spot was ~1 μm. Raw counts were collected over 20 seconds and were constant with time indicating that elemental drift was negligible. Detection limits for probe analyses are ~0.02 oxide weight percent. Additionally, backscattering electron (BSE) images of the rocks and soils were obtained using the microprobe.

Carbon-coated petrographic thin sections of rock samples were used for microprobe analyses. Soil samples were dried in an oven at 60°C for 24 hours, mounted onto a glass slide using epoxy, and heated to 100°C until the epoxy cured. An initial cut of each section using a petrographic saw was made followed by a second infusion of epoxy to ensure total impregnation. Finally, each section was cut, polished, and carbon-coated for electron microprobe measurements.

Soil chemistry.—Soils were analyzed for pH, electrical conductivity (EC (dS m^{-1})), particle size, ammonium acetate extractable cations, organic carbon, total nitrogen, and elemental composition. The pH was determined using a 1:1 mixture of soil to deionized water. Electrical conductivity (EC) was determined on 2 milliliters of a soil solution extract. Particle size of the soil was measured using the hydrometer method as described by Gee and Bauder (1986). These analyses were performed at the Utah State University Analytical Laboratory.

Ammonium acetate was used to measure the concentration of extractable K, Ca, Mg, and Na within the soil. The procedure involved weighing 2 grams of soil and adding 25 milliliters of ammonium acetate (20 M NH_4OAc) followed by mixing on an orbital shaker for 30 minutes. The solution was filtered using a Whatman #42 filter paper (pore size: 2.5 μm). Potassium, Ca, Mg, and Na concentrations were analyzed using atomic absorption spectrophotometry (AAS).

Organic carbon was measured using the Walkley-Black titration method (Mebius, 1960). Approximately 0.5 grams of sediment was weighed and reacted with 5 milliliters of 2.0 M potassium chromate ($K_2Cr_2O_7$) followed by the rapid addition of 10 milliliters concentrated sulfuric (H_2SO_4) acid. The bottle was cooled for 30 minutes at room temperature and diluted with 100 milliliters of deionized water. Next, 0.30 milliliters of 0.025 M ortho-phenanthroline-ferrous solution was added and the solution titrated to the endpoint using 1.0 M ferrous sulfate ($FeSO_4$).

Total nitrogen of soil samples was obtained using an automated combustion method as described by Sweeny (1989). Approximately 150 milligrams of air-dried and sieved (40 mesh) soil was placed in a tin foil encapsulating cup. A Leco total nitrogen analyzer with resistance furnace was then used to determine total nitrogen.

Major and minor element concentrations for soil and rock samples were obtained by completely dissolving the samples using a mixture of hot, concentrated nitric, perchloric, and hydrofluoric acids. Elemental concentrations were measured in the supernatant using inductively coupled atomic emission spectroscopy (ICP-AES). Standards were ± 5 mg kg^{-1} of their known values. These analyses were completed at Chemex Laboratory (Vancouver, Canada). Soil samples were dried and sieved (< 2 mm) before analysis in order to remove the larger rock fragments. Additionally, total element concentrations for > 2 millimeters, sand, silt, and clay size fractions were obtained for each sample collected at Site JR3.

X-ray Diffraction and Clay-size Mineral Identification

X-ray diffraction (XRD) analyses were conducted on the clay-size fraction (< 2 μm) from Site JR3 using a Siemens Diffraktometer D5000 at the University of Idaho. The clay-size fraction was isolated using a suspension method described by Vaniman (2001). Organic matter and calcium carbonate were removed from the clays using a concentrated hypochlorite solution (Kunze and Dixon, 1986). Crystalline and non-crystalline iron oxides were removed using a citrate-sodium bicarbonate-sodium dithionite (CBD) solution (Kunze and Dixon, 1986). The remaining phyllosilicate minerals were analyzed using a series of treatments including: 1) magnesium-saturation (2 M MgCl and 2 M MgAOC) and air drying, 2) magnesium-saturation and glycolation (1 % glycerol-ethanol solution), 3) potassium-saturation (1 M KCl) and air drying, and 4) potassium (1 M KCl) saturation followed by heating to 500°C (Whittig and Allardice, 1986). X-ray diffraction patterns were collected between 2θ values of 2.0° – 35.0° and 2.0° – 15.0°, with a generator potential of 30 kV, a generator current of 22 mA (using CuKα radiation), a Ni filter, and a scan speed of 1° min^{-1}. The software package JADE was used for XRD data analysis and mineral identification.

X-ray Absorption Spectroscopy

In-situ fluorescence yield X-ray absorption near-edge structure (XANES) spectroscopy at the Cr K-edge (edge inflection point is 5989 eV for Cr(0)) was conducted at the Stanford Synchrotron Radiation Laboratory (SSRL), Stanford, California, using beamlines 4 - 1 and 4 - 3. A Si(220) monochromator and a Ge-detector were used and three scans were collected for each XANES analysis. Soil and rock samples from Site JR3 were prepared by removing the > 2 millimeter fraction and crushed to a fine powder. Samples were loaded into a plastic sample holder and covered with Mylar tape.

Elemental mapping of three samples were completed at SSRL on Beamline 11-2 using X-ray absorption spectroscopy (XAS). A Si(220) monochromator with a 6 μm focusing capillary was used and fluorescence intensity was monitored with a Ge detector. Samples were prepared similar to those used for mineral identification using the electron microprobe; however, the thickness of the sample was decreased to < 20 μm.

Sequential Extraction Procedure

Sequential extraction experiments were completed on 2 grams, < 2 millimeter sieved soils (Diablo clay from Site 1 at 10 cm depth and serpentine soil from Site 2 at 4 cm depth) in three steps. The exchangeable fraction was obtained using a barium chloride (1mM $BaCl_2$) solution for 1 hour at 25°C (Kunze and Dixon, 1986). The Fe-crystalline oxide fraction was obtained by reacting the solids with a hydroxylamine-hydrochloride/acetic acid (1.0 M $NH_2OH \cdot HCl$ in 25 percent (V/v) HOAc) solution for 6 hours at 60°C (Chester and Hughes, 1967). The silicate fraction was obtained by reacting the solids with concentrated hydrofluoric acid (10 M HF) for 16 hours at 25°C. Trace element concentrations for each extraction were measured on the supernatant using inductively coupled plasma optical emission spectrophotometry (ICP-OES). All analyses were completed in triplicate. Additionally, sequential extraction experiments were completed on 2 grams, 106 to 250 millimeters sieved, ultrasonically cleaned commercial grade chromite (MSDS No. 302-1. WHMIS Class: D2A) using the same procedures listed above. The stoichiometric composition of chromite obtained using the electron microprobe is $(Fe_{0.46}Mg_{0.52}Mn_{0.02})(Cr_{0.61}Al_{0.29}Fe_{0.10})_2O_4$. Chromite was imaged after each sequential extraction using a JEOL 5600LV environmental SEM equipped with an EDAX thin-window energy dispersive X-ray detector.

TABLE 1

Whole rock elemental concentrations of serpentines (fig. 1B), chert, and sandstone*

Elemental Concentrations		Location of Serpentinites†							Chert‡	Sandstone‡
		JR1	JR3E	JR6E	Site 2	Site 5	Site10	JR3		
Al	wt. %	0.2	0.8	0.3	0.27	2.2	1.07	0.24	0.79	0.27
Ca	wt. %	0.26	0.07	0.05	0.03	0.46	0.13	0.03	0.01	<0.01
Co	mg kg^{-1}	101	99	100	99	155	217	97	1	<1
Cr	mg kg^{-1}	580	2,280	1,510	1,840	1,945	2,090	1,465	10	<1
Fe	wt. %	3.03	7.1	6.09	5.81	7.6	11.06	5.12	0.41	0.24
K	wt. %	0.01	0.31	0.99	<0.01	<0.01	0.01	<0.01	0.29	0.08
Mg	wt. %	12.2	13.4	15.4	13.36	5.24	8.04	11.2	0.14	0.34
Mn	mg kg^{-1}	495	800	155	730	1,375	1,860	460	110	85
Na	wt. %	1.81	0.06	0.93	<0.01	<0.01	<0.01	<0.01	0.01	0.01
Ni	mg kg^{-1}	2,037	1,545	3,321	3,510	3,020	3,960	2,740	20	9

*Total digestion ICP-AES analyses
†Serpentinites are dominantly composed of the minerals serpentine, chlorite, talc, and spinels.
‡See figure 1B for sample locations.

RESULTS

Serpentinite Mineralogy

The average serpentinite at Jasper Ridge is composed of serpentine (mainly lizardite and antigorite; (70 %), chlorite (15 %), talc (10 %), magnetite (4 %), and chromite (1 %) based on petrographic and microprobe observations of five samples (JR3E, JR6E, 5, 10, and JR3); however, brucite has been reported as a major constituent in related Franciscan Complex serpentinites (Hostetler and others, 1966). Other minerals identified include olivine, augite, and enstatite. Although the serpentinite mineralogy is relatively simple, the modes and textures of the minerals present in the rock vary significantly from site to site. In table 1, whole rock serpentinite compositions from Sites JR1, JR3E, JR6E, 2, 5, 10, and JR3 are listed. The average Cr concentration of

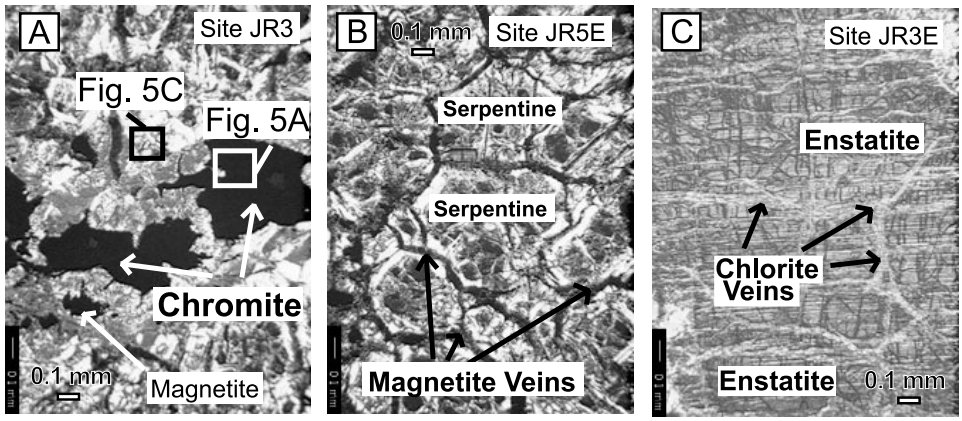

Fig. 3. Petrographic images illustrating the varying serpentinite textures at Sites (A) JR3, (B) JR5E, and (C) JR3E. For reference to site locations see figure 1B.

TABLE 2A

Selected Cr-bearing minerals and compositions in oxide weight percent in serpentinite rock at Jasper Ridge*

	Chlorite	Enstatite	Augite	Chromite	Cr-Magnetite	Chromite/Silicate†
SiO_2	37.38	54.63	52.22	0.00	0.24	10.53
Al_2O_3	5.52	4.77	5.16	50.59	1.82	3.95
NiO	0.01	0.1	0.0	0.3	0.0	0.52
FeO‡	7.62	6.14	2.39	14.46	79.19	50.42
MnO	0.09	0.15	0.09	0.42	1.40	1.82
Cr_2O_3	0.24	0.60	0.99	15.84	16.05	19.39
MgO	33.37	33.05	15.60	18.69	0.24	6.05
CaO	0.23	0.50	23.48	0.00	0.00	0.19
Na_2O	0.00	0.01	0.50	0.00	0.01	0.08
K_2O	0.00	0.00	0.01	0.00	0.00	0.11
Total	84.46	99.94	100.48	100.27	98.94	93.07
			Formula Unit Compositions			
Si	3.70	0.94	1.89	0.00	0.01	—
^{IV}Al	0.30	0.06	0.11	0.00	0.00	—
^{VI}Al	0.35	0.04	0.11	1.57	0.08	—
Ni	0.00	0.00	0.00	0.01	0.00	—
Fe^{2+}	0.63	0.10	0.07	0.30	2.32	—
Mn	0.01	0.00	0.00	0.01	0.04	—
Cr	0.02	0.01	0.03	0.33	0.48	—
Mg	4.93	0.85	0.84	0.73	0.01	—
Ca	0.02	0.01	0.91	0.00	0.00	—
Na	0.00	0.00	0.04	0.00	0.00	—
K	0.00	0.00	0.00	0.00	0.00	—
O	14.00	3.00	6.00	4.00	4.00	—

*Electron microphobe analyses
†Chromite/silicate is also referred to as CSM.
‡Fe^{3+} is present; however, all conversions are based on Fe^{2+}.

the serpentinites is ~1700 mg kg^{-1} (table 1). Iron (~7 wt. %), Mg (~ 11 wt. %), Ni (~3000 mg kg^{-1}), and Co (~100 mg kg^{-1}) concentrations are also elevated in the serpentinite relative to the chert and sandstone bedrock adjacent the main serpentinite body (fig. 1B and table 1).

A range of rock and mineral textures are petrographically evident in the serpentinite at Jasper Ridge (fig. 3). No foliations or lineations are observed in the serpentinite (fig. 3A) obtained from the bottom of the soil pit excavated at Site JR3 (fig. 1B). Subhedral chromite and magnetite grains are randomly interspersed amongst the serpentine matrix (fig. 3A). In serpentinite obtained in outcrop at Site JR5E (fig. 1B), a 'crocodile skin' texture is produced by thin, irregular veins of fine-grained subhedral magnetite separating serpentine grains (fig. 3B). In figure 3C, numerous crosscutting veins of chlorite occur in orthopyroxene and define the foliation of the rock in outcrop at Site JR3E (fig. 1B). The numerous crosscutting microscopic veins, random foliation patterns (or the lack thereof), and subhedral oxide grains suggest the Jasper

TABLE 2B

Representative Cr-bearing minerals and compositions in oxide weight percent in serpentine soil at Jasper Ridge*

	CSM	Chromite	Cr-Magnetite
SiO_2	19.40	0.57	2.67
Al_2O_3	5.59	10.59	3.81
NiO	0.14	0.01	0.04
FeO†	26.29	22.59	52.44
MnO	1.55	1.54	4.19
Cr_2O_3	18.78	55.77	32.37
MgO	16.68	9.16	2.88
CaO	0.15	0.01	0.05
Na_2O	0.06	0.01	0.01
K_2O	0	0.08	0.09
Total	88.64	100.33	98.55
	Formula Unit Compositions		
Si	—	0.02	0.10
^{IV}Al	—	0.42	0.17
^{VI}Al	—	0.00	0.00
Ni	—	0.00	0.00
Fe^{2+}	—	0.63	1.48
Mn	—	0.04	0.13
Cr	—	1.47	0.96
Mg	—	0.46	0.16
Ca	—	0.00	0.00
Na	—	0.00	0.00
K	—	0.00	0.00
O	—	4.00	4.00

*Electron microprobe analyses
†Fe^{3+} is present; however, all conversions are based on Fe^{2+}.

Ridge serpentinite has undergone extensive physical and chemical alteration typical of most serpentinites.

Microprobe analyses of minerals in the serpentinite demonstrate that the main Cr-bearing phases are chlorite, enstatite, augite, Mg-Al chromite, Cr-magnetite, and a chromite-silicate mixture (defined in the following paragraph). Selected compositions for these minerals are listed in order of their Cr concentrations in table 2A. Chlorite contains the least Cr, whereas, the chromite-silicate mixture is the most enriched with respect to Cr. Figure 4 shows correlations of Cr content relative to Al, Fe, Mg, and Si in order to provide insight into the serpentinite mineralogy and to aid in evaluating trends of Cr substitution.

A fine-grained mixture of spinel (chromite and/or Cr-magnetite) and a silicate contains the highest Cr concentration in the serpentinite at Jasper Ridge (table 2A; shown in fig. 5A and 5B). This fine-grained mixture will be referred to here as the chromite-silicate mixture (CSM) with chemical properties similar to those in table 2A and figure 4. CSM is common around the rims of protolith chromite grains and a number of the larger (~0.5 mm) Cr-magnetite grains in the serpentinite. The microcrystalline phase responsible for contributing Si to these analyses is possibly

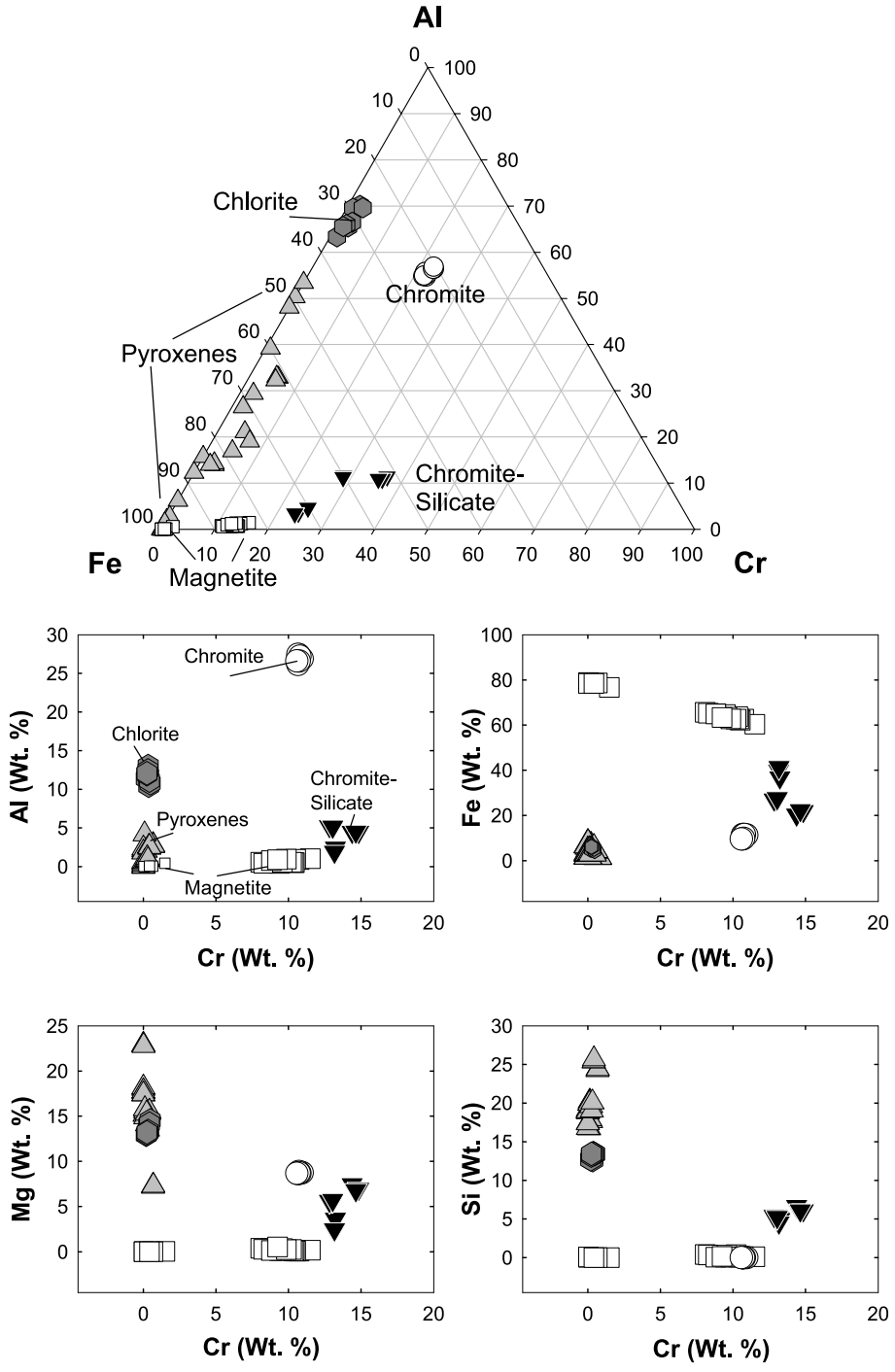

Fig. 4. Compositions of Cr-bearing minerals in the serpentinite at Jasper Ridge comparing microprobe analyses of Cr versus Al, Fe, Mg, and Si in weight percent. Chromite (circle), Cr-magnetite (square), chromite/silicate or CSM (down triangle), chlorite (hexagon), and pyroxenes (up triangle) analyses are shown on each correlation diagram.

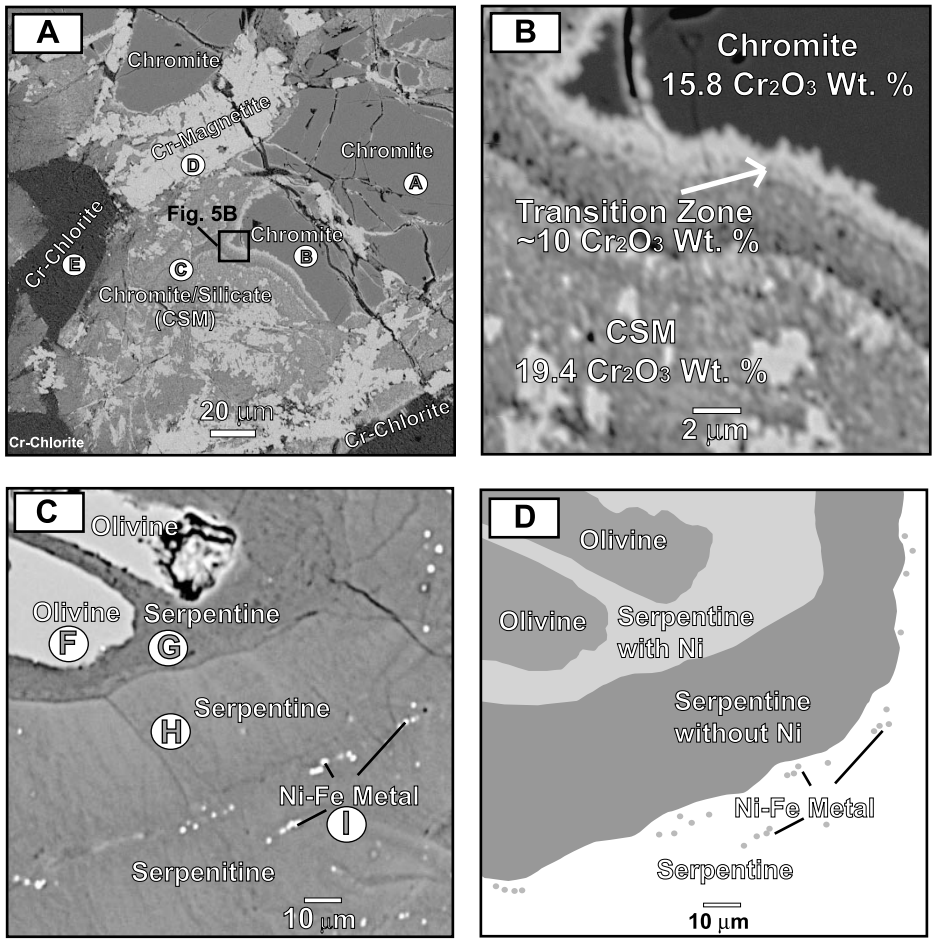

Fig. 5. Images of the serpentinite bedrock at Site JR3 demonstrating the mineralogy and Cr-bearing phases. Microprobe analyses are indicated by circled letters and these values are in table 3. (5A) Backscattering electron image demonstrating several Cr-bearing phases present including chromite, Cr-magnetite, CSM, and Cr-chlorite from figure 3A. (5B) Magnified image shown in figure 5A demonstrating the fine-grained texture of CSM. Additionally, Cr_2O_3 weight percent values are shown for chromite, the depletion zone, and CSM. (5C) Image of Ni-bearing phases present in the bedrock including olivine, serpentine, and Ni-Fe alloy from figure 3A. (5D) Cartoon illustrating the mineralogical and chemical changes present in 5C.

chlorite due to similarities of false colors generated by backscattering electron (BSE) images and chlorite commonly rimming CSM. Microprobe analyses of CSM listed in tables 2 and 3 are considered as mixtures of several mineral phases due to the fine-grained texture (< 1 μm). Chromium concentrations range from 12 to 16 Cr weight percent in this phase. CSM is chemically distinct from the chromite and magnetite as shown in figure 4.

The chemical compositions of protolith chromite exhibit little to no variation in any of the serpentinites collected at Sites 2, JR3E, JR4E, JR5E, JR6E, JR7E, and JR3 (table 2A and fig. 4). Chromite contains low Fe (~9 wt. %), high Mg (~9 wt. %), and high Al (~26 wt. %) compared to Cr-magnetite. The average Cr concentration for chromite is ~12 Cr weight percent. Additionally, chromite grains are irregular and subhedral suggesting that they have undergone significant alteration during metamorphism.

TABLE 3

Mineral compositions in oxide weight percent of minerals identified by letters A–L in figures 5 and 6.*

	A	B	C	D	E	F	G	H	I	J	K	L
	Chromite	Chromite	CSM	Magnetite	Chlorite	Olivine	Serpentine	Serpentine	Ni-Fe-Metal	Cr-Magnetite	CSM	Chlorite
SiO_2	0	0	10.53	0	34.07	40.46	36.88	40.74	5.91†	0.21	11.43	28.55
Al_2O_3	50.59	51.62	3.95	0.34	11.14	0.00	3.97	0.85	0.54	1.65	9.80	22.93
NiO	0.28	0.31	0.52	0	0.04	0.37	0.37	0	53.02†	0	0	0
FeO‡	14.46	14.52	50.42	99.92	12.20	9.01	2.62	4.53	17.53†	81.69	34.98	8.06
MnO	0.42	0.44	1.82	0	0.08	0.10	0	0	0	1.07	1.50	0.0
Cr_2O_3	15.84	15.76	19.39	1.25	0.71	0.01	0	0	0	13.69	19.05	0.39
MgO	18.69	18.69	6.05	0.03	29.2	48.95	38.48	37.55	23.21	0.64	12.17	28.28
CaO	0	0	0.19	0	0	0	0	0	0	0	0	0
Na_2O	0	0	0	0	0	0	0	0	0	0	0	0
K_2O	0	0	0	0	0	0	0	0	0	0	0	0
H_2O	—	—	—	—	12.00	—	16.00	16.00	—	—	—	12.00
Total	100.27	101.36	93.07	101.64	99.44	98.91	98.34	99.72	100.25	98.97	88.97	100.28
							Formula Unit Composition					
Si	0.00	0.00	—	0.00	3.28	1.00	1.84	2.00	5.91	0.01	—	2.69
^{IV}Al	0.00	0.00	—	0.00	0.72	0.00	0.00	0.00	0.00	0.00	—	1.31
^{VI}Al	1.57	1.59	—	0.02	0.58	0.00	0.23	0.05	0.54	0.07	—	1.23
Ni	0.01	0.01	—	0.00	0.00	0.01	0.01	0.00	53.02	0.00	—	0.00
Fe^{2+}	0.30	0.29	—	2.94	0.84	0.19	0.11	0.19	17.53	2.39	—	0.59
Mn	0.01	0.01	—	0.00	0.00	0.00	0.00	0.00	0.00	0.03	—	0.00
Cr	0.33	0.32	—	0.04	0.06	0.00	0.00	0.00	0.00	0.41	—	0.03
Mg	0.73	0.73	—	0.00	4.19	1.80	2.85	2.74	23.21	0.04	—	3.97
Ca	0.00	0.00	—	0.00	0.00	0.00	0.00	0.00	0.00	0.00	—	0.00
Na	0.00	0.00	—	0.00	0.00	0.00	0.00	0.00	0.00	0.00	—	0.00
K	0.00	0.00	—	0.00	0.00	0.00	0.00	0.00	0.00	0.00	—	0.00
O	4.00	4.00	—	4.00	14.00	4.00	7.00	7.00	0.00	4.00	—	14.00

*Electron microprobe analyses, †elemental metal, ‡Fe^{3+} is present; however, all conversions are based on Fe^{2+}.

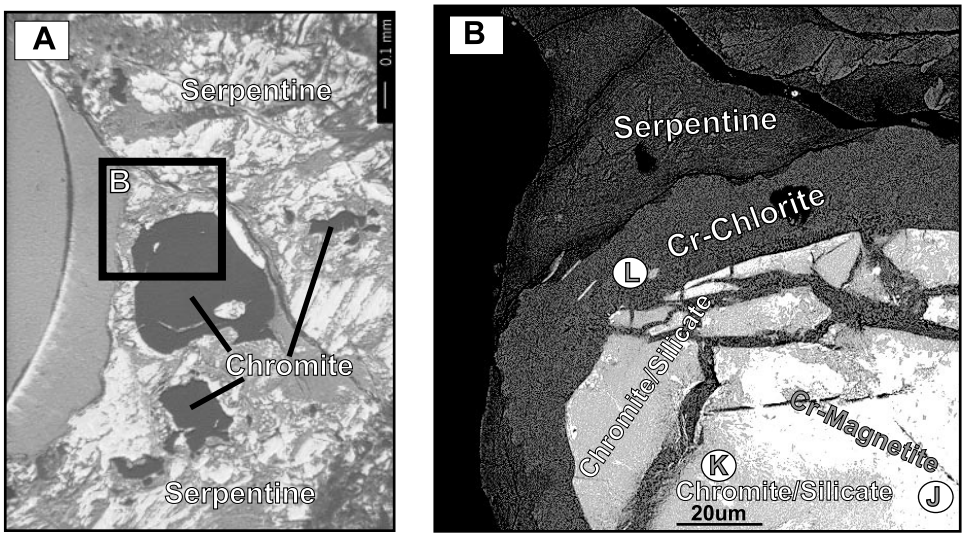

Fig. 6. Images of a Cr-chlorite and Cr-magnetite assemblage in the serpentinite bedrock. (6A.) Petrographic image of the bedrock at Site 4 (figure 1B). (6B.) Backscattered electron image demonstrating the common occurrence of Cr-chlorite encompassing chromite grains. Microprobe analyses are indicated by circled letters and are located in table 3.

Chromium concentrations in the magnetite vary depending on the proximity and degree of alteration of the chromite (table 2A and fig. 4). Magnetite grains with less than 2 Cr weight percent are common in veinlets in serpentinite not formed adjacent chromite, whereas, magnetite with 8 to 12 Cr weight percent were formed proximal or adjacent to chromite. Chromium-enriched magnetite is also referred to as ferrite-chromite in the literature (Spangenberg, 1943; Burkhard, 1993).

Chlorites and pyroxenes contain minor concentrations of Cr (< 1 wt. %; table 2A). Aluminum, Fe, and Mg concentrations varied in the pyroxenes; however, the majority of chlorites are relatively similar in composition (fig. 4). Chlorites are more abundant in the serpentinite compared to the pyroxenes and both minerals were subhedral and distributed over the entire sampling area (fig. 1B).

Backscattering electron (BSE) images of what appeared to be a petrographically opaque single chromite grain in figure 3A demonstrates that chromite has been metasomatically altered resulting in the formation of Cr-magnetite, Cr-chlorite, and CSM (fig. 5A). Represented compositions for these minerals (indicated by letters in figure 5A) are listed in table 3. Magnifying the chromite and CSM from figure 5A demonstrates the fine-grained texture of CSM and an alteration rim (transition zone) is also seen along the chromite edge (fig. 5B). This alteration rim is depleted in Cr with respect to the chromite as shown in figure 5B.

In figures 3A and 5C, Ni was identified in three phases in the bedrock including olivine (F: 0.3 Ni wt. %), serpentine (G and H: 0.3 and 0 Ni wt. %), and Ni-Fe (I: ~55 Ni wt. %) alloy (fig. 5C and 5D); their compositions are indicated by letters and listed in table 3. Alteration of the olivine resulted in the formation of < 10 μm Ni-Fe alloy grains shown in figure 5C. These Ni-Fe alloys form a corona surrounding the remaining olivine and the illustration in figure 5D highlights the minerals and chemical changes.

Chromite and Cr-magnetite alteration leading to the paragenesis of CSM and Cr-chlorite is common in the serpentinites at Jasper Ridge. The petrographic image in figure 6A and its corresponding BSE image in figure 6B illustrate Cr-magnetite (originally protolith chromite) partially altering to CSM and Cr-chlorite. The chemical

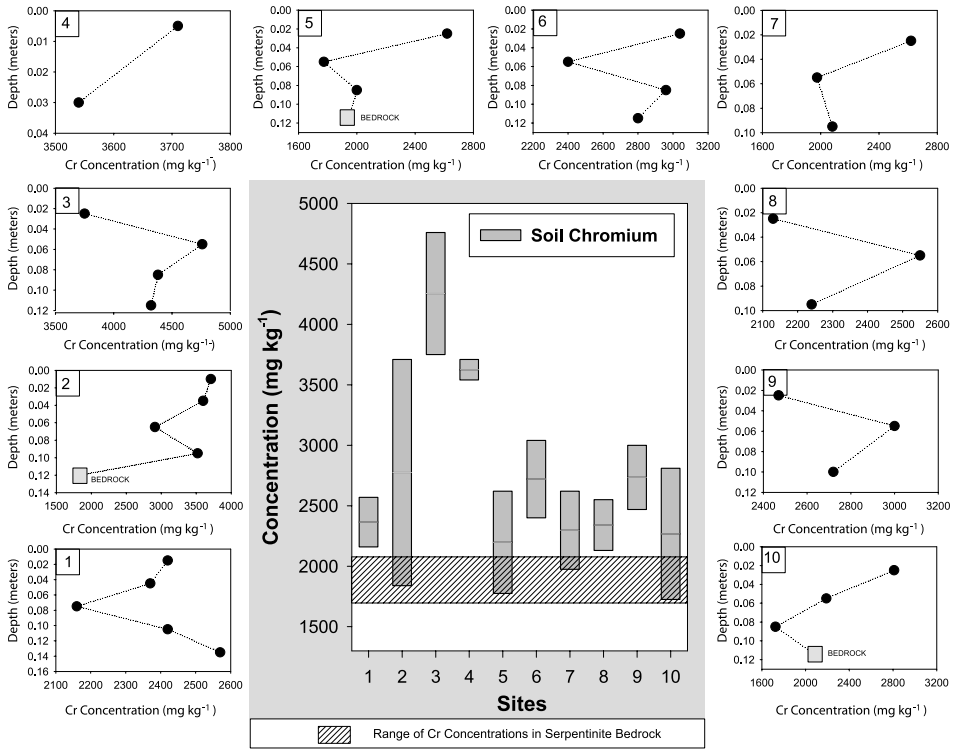

Fig. 7. Highest and lowest Cr concentrations (mg kg^{-1}) at each site in the serpentine soil 500 meters transect shown in figure 1B. Samples included soils at various depths (m) and bedrock from each site. The average Cr concentration for the Jasper Ridge serpentinite is marked on the central figure. Chromium concentrations versus depth (m) at each site (noted in the upper left corner) outline the main diagram.

compositions of each mineral (indicated by letters in figure 6B) are listed in table 3. CSM appears to marginally and metasomatically replace Cr-magnetite and is enriched by ~2 Cr weight percent. Chromium-chlorite is present in microcracks in Cr-magnetite and encompasses the entire Cr-magnetite and CSM grain. Serpentine minerals adjacent the Cr-chlorite contains no measurable Cr.

Distribution of Chromium in Serpentine Soils

Serpentine soils and underlying bedrock were collected at ten sites along a 500 meter transect extending the length of the main serpentine body as shown in figure 1B. The range of Cr concentrations at each site (center) and Cr concentrations with respect to depth (periphery) are shown in figure 7 and soil analyses are listed in table 4. Bedrock Cr concentrations for Sites 2, 5, and 10 are also shown in these plots (fig. 7). Chromium enrichment does not appear to be consistently found at a particular depth or soil horizon for any of the sites. Sites 3, 9, and 10 demonstrate a Cr maximum at approximately 0.06 meters; however, Sites 1, 2, 5, and 6 exhibit a Cr minimum at roughly the same depth. The highest soil Cr concentration in the soil along the transect is 4,760 mg kg^{-1} at Site 3 at 0.06 meter depth. The lowest soil Cr concentration is 1,725 mg kg^{-1} at Site 10 at 0.085-meter depth. The average bedrock Cr concentration is ~2,000 mg kg^{-1} (fig. 7; table 4). It is important to note that Site 1 consists of Diablo clay, not serpentine soil; however, this site is located adjacent and down-slope of the main serpentinite body. From these observations it is apparent that there are no systematic trends in soil Cr concentrations with respect to the location of the site and

TABLE 4

Bulk soil elemental concentrations for soils and bedrock collected along the transect (fig. 1B)*

Sites Locations	Samples	Depth (meters)	Cr (mg kg^{-1})	Ni (mg kg^{-1})	Mn (mg kg^{-1})	Co (mg kg^{-1})	Al (%)	Fe (%)	Ca (%)	Mg (%)
1	COI03	0.015	2,420	1,590	1,325	118	4.64	5.65	0.65	3.52
	COI36	0.045	2,370	1,630	1,600	138	4.67	5.5	0.63	3.56
	COI69	0.075	2,160	1,755	1,670	144	4.71	6	0.64	3.65
	COI912	0.105	2,420	1,785	1,740	151	4.96	6.15	0.67	3.84
	COI1215	0.135	2,570	1,985	2,340	195	5.06	6.49	0.69	4.11
2	COII02	0.01	3,710	2,400	1,665	169	2.94	7.02	1.00	7.68
	COII25	0.035	3,600	2,290	1,625	162	2.75	6.73	0.93	7.43
	COII58	0.065	2,910	2,310	1,550	159	2.5	6.72	0.87	7.71
	COII811	0.095	3,520	2,350	1,595	158	2.76	6.93	0.93	7.66
	COIIBedrock	0.12	1,840	3,510	730	99	0.27	5.81	0.03	13.36
3	COIII14	0.025	3,750	2,930	1,655	190	1.78	8.97	0.62	7.62
	COIII47	0.055	4,760	3,050	1,850	178	1.78	9.4	0.56	8.05
	COIII710	0.085	4,380	3,410	1,930	216	2.16	10.44	0.7	7.97
	COIII1013	0.115	4,320	3,380	1,955	201	2.13	10.61	0.63	6.26
4	COIV01	0.005	3,710	2,970	1,915	214	2.09	9.09	0.53	7.81
	COIV15	0.03	3,540	2,710	1,725	195	1.81	8.01	0.43	7.92
5	COV14	0.025	2,620	2,350	1,330	150	2.46	6.51	0.63	5.26
	COV47	0.055	1,775	2,710	1,520	165	2.52	7.66	0.59	5.17
	COV710	0.085	2,000	3,090	1,830	195	2.25	7.37	0.57	5.83
	COVBedrock	0.115	1,945	3,020	1,375	155	2.2	7.6	0.46	5.24
6	COVI14	0.025	3,040	3,720	1,855	224	0.84	11.52	0.15	7.36
	COVI47	0.055	2,400	3,610	1,785	218	0.85	11.38	0.14	6.8
	COVI710	0.085	2,960	3,800	1,850	232	0.93	12.32	0.15	7.14
	COVI1013	0.115	2,800	3,860	1,800	224	0.85	11.64	0.14	7.39
7	COVII14	0.025	2,620	3,550	1,925	229	0.83	11.28	0.15	7.18
	COVII47	0.055	1,975	3,590	1,805	216	0.84	10.85	0.14	6.55
	COVII712	0.095	2,080	3,600	1,840	220	0.7	11.05	0.11	7.41
8	COVIII14	0.025	2,130	3,830	1,990	238	0.85	11.5	0.17	7.05
	COVIII47	0.055	2,550	3,720	1,865	228	0.85	10.99	0.17	7.14
	COVIII712	0.095	2,240	3,910	1,860	229	0.76	11.12	0.14	8.28
9	COIX14	0.025	2,470	3,480	1,890	227	1.04	12.01	0.23	5.79
	COIX47	0.055	3,000	3,830	1,595	205	0.84	10.8	0.13	8.42
	COIX713	0.1	2,720	3,710	1,845	221	1.11	12.08	0.17	5.51
10	COX14	0.025	2,810	3,740	1,760	218	1.29	11.4	0.17	6.75
	COX47	0.055	2,190	3,910	1,835	224	1.31	12.06	0.17	7.02
	COX710	0.085	1,725	3,370	1,595	192	1.1	10.61	0.14	6.35
	COXBedrock	0.115	2,090	3,960	1,860	217	1.07	11.06	0.13	8.04

*Total digestion ICP-AES analyses

depth. However, soil samples often contain higher concentrations of Cr with respect to their corresponding bedrock and to the average Cr concentration of ultramafic rocks (1600 mg kg^{-1}; Green, 1972).

Trace metals including Ni, Mn, and Co were also analyzed in the serpentine soil for Sites 1 through 10 and the results are listed in table 4. Nickel concentrations range from 1,590 to 3,960 mg kg^{-1} and do not directly correspond to the changes in Cr concentrations with respect to depth (table 4). Nickel concentrations are lower than Cr concentrations from Sites 1 to 4. From Sites 5 to 10, Ni concentrations exceed those of Cr averaging ~3,600 mg kg^{-1}. Unlike Cr, Ni concentrations are equivalent or greater in the bedrock (~3,300 mg kg^{-1}) as compared to the soil (~3,200 mg kg^{-1}). Soil Mn concentrations at each site are relatively uniform at ~1,800 mg kg^{-1} with little to no variation with depth (table 4). Cobalt concentrations do not exceed 238 mg kg^{-1}

(table 4) and are relatively uniform (~200 mg kg^{-1}) with respect to location along the transverse and depth at each site.

Major elements including Al, Fe, Ca, and Mg are listed for the serpentine soils along the transect with respect to depth in table 4. Aluminum, Fe, Ca, and Mg concentrations in the soils at each site are similar with the exception of Site 1 (Diablo clay). Aluminum concentrations in the Diablo clay are ~4.6 weight percent, whereas, the serpentine soils contain less than 2 weight percent Al (table 4). Iron and Mg concentrations are also low, < 6.5 weight percent and < 4.11 weight percent respectively, in the Diablo clay compared to Fe (> 8 wt. %) and Mg (> 6 wt. %) concentrations in the serpentine soil (table 4). Calcium concentrations are low (< 1 wt. %) for all the serpentine soils and even the Diablo clay (table 4). With this understanding of the chemical characteristics of the serpentine soil at Jasper Ridge, Site JR3 (fig. 1B) was chosen for a detailed chemical study to examine the factors governing the chemistry of Cr in the soil.

Serpentine Soil Chemistry and Mineralogy at Site JR3

Soil chemistry.—Chemical properties (pH, electrical conductivity, organic carbon, nitrogen, and ammonium acetate extractable cations) and textures for four soil samples from Site JR3 are listed in table 5. The pH of the soil is near neutral (pH from 6.71 to 6.98) and increases slightly with respect to depth. Electrical conductivities (EC) in the soil ranges from 0.3 to 0.9 dS m^{-1}, a range indicative of relatively few dissolved salts and/or major dissolved inorganic solutes. The organic carbon content of the soil is 3.2 percent at the surface and decreases with depth to 1.0 percent near the bedrock. Total nitrogen for the samples ranged from 0.03 percent to 0.64 percent. Ammonium acetate extractable Ca, K, Mg, and Na are listed in table 5. The extractable concentration of both Ca and K decrease with depth, whereas, there is no apparent trend associated with the concentrations of Mg and Na. The serpentine soil textures are dominantly clay loams; however, the texture is a sandy clay loam near the bedrock.

Whole soil samples and size fractions including > 2 millimeter, sand (2-0.02 mm), silt (0.02-0.002 mm), and clay (< 2 μm) size fractions with respect to depth were chemically digested and analyzed for total trace metal concentrations, listed in table 6, to determine if the abundance of Cr was linked to a particular size fraction (the percent of sand, silt, and clay size fractions are reported in table 5). Additionally, Ni, Mn and Co concentrations with respect to depth and size fraction are also presented in table 6. Total and > 2millimeter size fraction Cr concentrations are similar at the top and bottom of the soil profile ranging from 3,297 to 5,976 Cr mg kg^{-1}. Chromium concentrations exceed detections limits (> 10,000 mg kg^{-1}) for the sand-size fraction. It is important to note that the sand-size fraction corresponds to the size of most chromite grains observed in the serpentinite. Chromium in the clay fractions is low (~1000 mg kg^{-1}) compared to the other size fractions; however, these concentrations are still enriched compared to non-serpentine soils.

In table 6, Ni concentrations are enriched in the clay-size fraction with values ranging from 2,840 to 2,920 mg kg^{-1}. The silt-size fractions have the lowest Ni concentrations (~1,800 mg kg^{-1}). Manganese concentrations are slightly elevated relative to total Mn in the sand-size fraction with values ranging from 1,728 to 2,701 mg kg^{-1}. The clay-size fraction is the least Mn enriched size-fraction with concentrations at ~1,200 mg kg^{-1}. Cobalt concentrations are elevated in the sand-size fraction with values ranging from 159 to 241 mg kg^{-1} and concentrations in the > 2 millimeter, silt, and clay-size fractions are similar to the total (~150 mg kg^{-1}).

Soil Cr-bearing minerals.—Chromium-bearing minerals in the soil identified using the electron microprobe include chromite, Cr-magnetite, and CSM. Chromium concentrations in soil chromite, Cr-magnetite, and CSM are graphically shown in figure 8 as a function of Al, Fe, Mg, Si, and Al+Fe in weight percent. Representative analyses of

TABLE 5

Chemical and physical properties of the soil at Site JR3*

Sample	Depth (cm)	pH	EC dS m^{-1}	Organic Carbon —%—	LECO Nitrogen —%—	NH_4OAc-extractable Ca	K	Mg	Na	—Hydrometer— Sand	Silt	Clay	Texture
						——— mg kg^{-1} ———				%	%	%	
JR305	2.5	6.71	0.4	3.2	0.12	505	236.6	3291	35.5	36	31	33	Clay Loam
JR3515	10	6.83	0.9	1.9	0.64	420.5	81.76	3343	23.92	36	30	34	Clay Loam
JR31530	22.5	6.88	0.3	1.2	0.03	372.5	49.03	3750	23.05	36	33	31	Clay Loam
JR33045	37.5	6.98	0.7	1.0	0.03	287.3	36.65	3388	25.49	46	24	30	Sandy Clay Loam

*See Methods Section for more details.

TABLE 6

Representative trace metal concentrations for different size fractions as a function of depth at Site JR3*

Sample	Depth (cm)	Total	> 2mm Fraction	Sand	Silt	Clay
			Chromium (mg kg^{-1})			
JR305	2.5	4,906	5,086	>10,000	4,565	988
JR3515	10	5,976	4,678	8,284	4,000	1,115
JR31530	22.5	5,222	4,206	>10,000	4,133	980
JR33045	37.5	3,477	3,297	>10,000	4,571	956
			Nickel (mg kg^{-1})			
JR305	2.5	1,935	2,050	1,660	1,305	2,920
JR3515	10	2,180	2,050	1,980	1,325	2,920
JR31530	22.5	2,190	2,120	1,835	1,370	2,880
JR33045	37.5	2,090	2,140	1,740	1,285	2,840
			Manganese (mg kg^{-1})			
JR305	2.5	1,319	1,571	1,728	1,301	1,210
JR3515	10	1,664	1,601	2,701	1,471	1,254
JR31530	22.5	1,639	1,626	2,217	1,599	1,231
JR33045	37.5	1,222	1,226	1,781	1,405	1,170
			Cobalt (mg kg^{-1})			
JR305	2.5	128	146	159	134	131
JR3515	10	155	145	241	147	132
JR31530	22.5	152	147	194	162	128
JR33045	37.5	125	124	159	141	122

*Total digestion ICP-AES analyses

the Cr-bearing soil minerals are listed in table 2B. Compositions of soil chromite in figure 8 are chemically distinct from those identified in the protolith in figure 4. Chromium concentrations in soil chromites range from 22 to 37 Cr weight percent and contain minor concentrations of Al and Mg. Values for chromite in the serpentinite bedrock (table 2A and fig. 4) and the $FeCr_2O_4$ end-member are also shown in figure 8. The dashed lines in figure 8 connect Jasper Ridge bedrock chromite (fig. 4) and stoichiometric $FeCr_2O_4$ where it can be seen that compositions of soil chromite lie close to these tie lines. Overall, soil chromite demonstrates a decrease in Al and Mg and an increase in Fe relative to Cr compared with protolith chromite. Soil Cr-magnetites contain between 7 and 20 Cr weight percent and are enriched in Cr compared to Cr-magnetites identified in the bedrock (fig. 4). Cr-magnetite, however, reveals a decrease in Fe relative to Cr. Minor concentrations of Si (< 2 wt. %) in the soil chromite and Cr-magnetite may represent slightly altered rims or contamination from sample preparation. Chromium concentrations in CSM maintain a consistent Cr concentration of ~11 Cr weight percent, similar to those found in the bedrock (~14 Cr wt. %). Soil CSMs with compositions between 8 and 12 Mg weight percent are more than likely associated with analyses containing more microcrystalline chlorite compared to soil CSMs with less than 2 Mg weight percent. Soil CSM appears to be less enriched with Si (< 14 wt. %) relative to those identified in the serpentinite (15 to 27 wt. %).

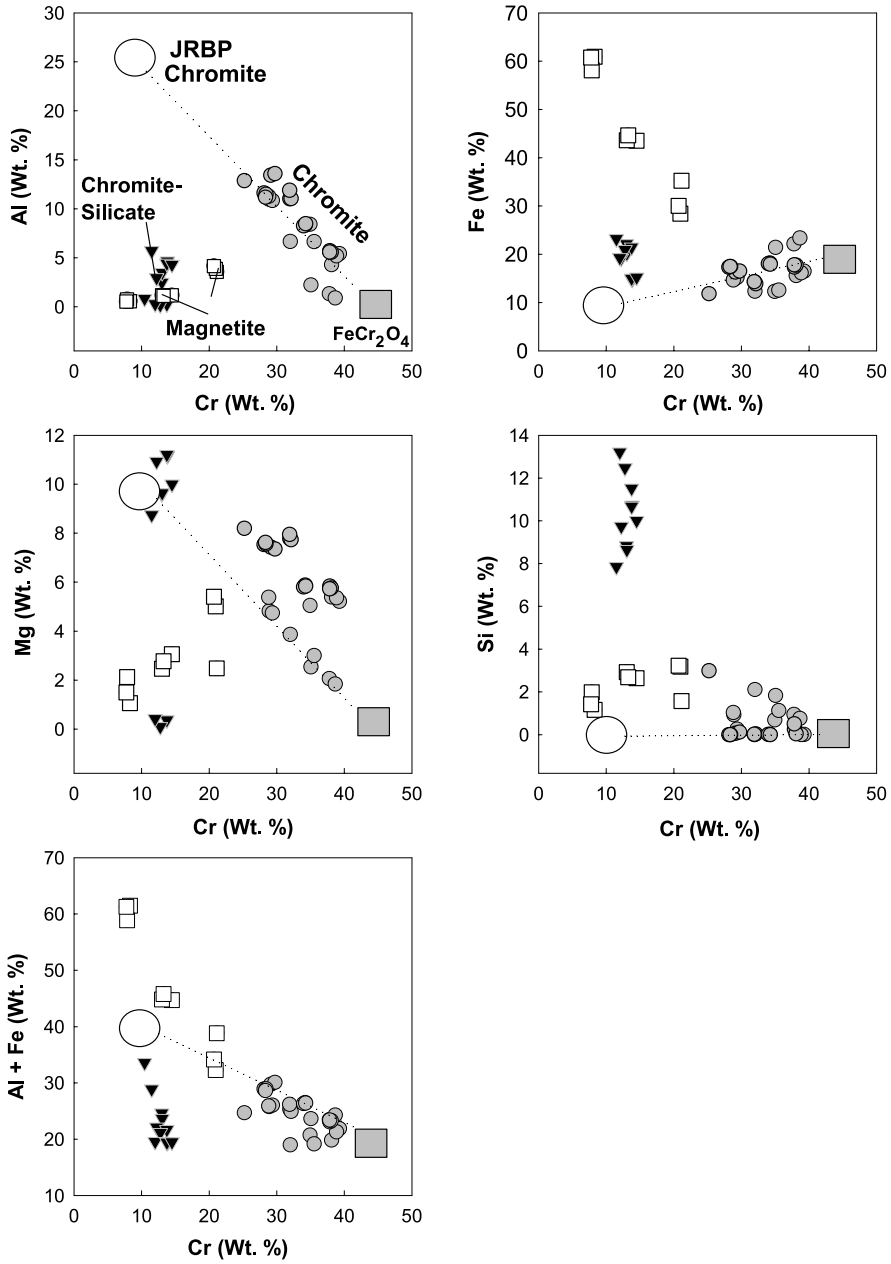

Fig. 8. Correlation diagrams of Cr-bearing minerals in the serpentine soil at Jasper Ridge comparing microprobe analyses of Cr versus Al, Fe, Mg, and Al+Fe in weight percent for chromite (circle), Cr-magnetite (square), and CSM (down triangle). Chromite from the bedrock is denoted by a larger circle and $FeCr_2O_4$ with a gray square.

The size of the Cr-bearing minerals varied significantly for each sample ranging from 10 μm up to 2 millimeters. The majority of chromite grains in the soil corresponds to the sand-size fraction and also varies from euhedral to subhedral with no discernable pattern. The sum of cations based on four oxygens for the chromite

and Cr-magnetite analyses range between 2.97 and 3.01, indicating these minerals are spinels, not (oxy)hydroxides. Compositions obtained for chromite and Cr-magnetite may represent alteration rims where weathering of the mineral in the subsurface environment has been most active. Based on BSE images of chromite and Cr-magnetite, we were not able to definitively identify whether these analyses in fact represent alteration rims.

Mineralogy of the clay-size fraction.—The clay-size fraction in the serpentine soil at Site JR3 was evaluated with respect to depth using XRD and specific chemical and heat treatments. The d-spacings (Å) and their relative intensities for each soil and treatment with respect to depth are listed in table 7. Figure 9 shows the XRD analyses for clay sample JR3515 (depth: 5 –1 5 cm) and these analyses are almost identical to the other clays examined at Site JR3. Additionally, table 8 from Whittig and Allardice (1986) is provided to interpret the X-ray diffraction analyses in table 7. For example, a d-spacing of ~14 Å is present in all the treatments indicating the presence of chlorite in the clay-sized fraction. Using an XRD analysis program, the clay-size fraction was determined to be composed of smectite, vermiculite, serpentine minerals (lizardite and antigorite), and chlorite (clinochlore and Cr-clinochlore). Smectite is the most abundant mineral in the clay-size fraction, whereas, Cr-chlorite is the least abundant. Overall, the d-spacings and relative intensities are similar despite the treatments and changes in depth (table 7 and fig. 9). These similarities indicate that the mineralogy of the clay-size fraction does not vary significantly in the soil column.

Chromium concentrations in the clay-size fractions are ~1,010 mg kg^{-1} (table 6). Smectite and vermiculite are possible Cr-bearing clay minerals in which isomorphic substitution of Cr(III) could occur in the dioctahedral sheet. Serpentine minerals (lizardite and antigorite) are not likely hosts of Cr based on crystallographic considerations and the absence of Cr in analyzed serpentine minerals in the bedrock (table 3). Clinochlore may also be a host for Cr in the brucite-like layer in the inter-layer region. Chromium-clinochlore is the only Cr-containing mineral identified in the clay-size fraction using XRD and Cr-clinochlore (Cr-chlorite) is also an abundant mineral identified in serpentinite protolith (tables 2 and 3; fig. 6).

XAS of chromium in relation to depth.—X-ray absorption spectroscopy (XAS) was used to deduce the oxidation state of Cr in serpentine soils and bedrock at Site JR3. The XANES (X-ray absorption near-edge structure) spectra demonstrate the absence of Cr(VI) in the soil column at Site JR3 (fig. 10) based on the lack of a pre-edge feature. The detection limit for Cr(VI) using this method is approximately ~20 mg kg^{-1}. Ultimately, XAS analyses did not detect Cr(VI) in any of the soil solids.

X-ray microprobe analyses of soil and rock samples (0 - 5cm depth, 5 - 10cm depth, and serpentinite) at Site JR3 were processed to map the relative concentrations of Fe and Cr; areas of elemental enrichment are identified by a violet color, areas of depletion by a blue color (fig. 11). Areas of Cr and Fe enrichment in figure 11 are localized with well-defined boundaries corresponding to grain edges, but these elements are not correlated in a well-defined trend. Minerals assigned to these areas of Cr and Fe enrichment were made based on petrographic and microprobe observations on the same thin section. For example, high Fe and no Cr is magnetite, whereas, high Fe and high Cr is either chromite or Cr-magnetite. Chromite, magnetite, and Cr-magnetite appear to be present in the serpentine soil at a depth between 0 to 5 centimeters (fig. 11A). In figure 11B, CSM is a possible mineral detected in the soil (depth: 5 - 10 cm) and the presence of magnetite is clearly seen due to the localized enrichment of Fe and no Cr. Iron and Cr spectra for the serpentinite were much more heterogeneous as compared to the soil samples and Cr concentrations appear be more

TABLE 7

X-ray diffraction analyses of the clay-sized fractions from site JR3*

JR305CLAY: Depth 0-5 cm							
Mg-Saturated, air-dried		**Magnesium+Glycerol**		**K-saturated, air-dried**		**K-saturated+Heat**	
d-spacing(Å)	*% Intensity*	*d-spacing(Å)*	*% Intensity*	*d-spacing(Å)*	*% Intensity*	*d-spacing(Å)*	*% Intensity*
14.39	100	18.33	100	12.74	100	13.91	100
7.31	17.9	14.32	43.1	7.32	64.5	10.47	10.5
7.1	21.6	9.41	16.3	7.1	41	8.38	8.38
4.74	10.1	8.47	14.1	4.75	25.7	7.26	7.26
3.56	12.5	7.3	27.1	3.65	26.4		
3.13	8.3	7.12	24.8	3.55	29.9		
		4.73	14.3	3.13	25.7		
		3.64	13.1				
		3.55	19.3				
JR3515CLAY: Depth 5- 15cm							
Mg-Saturated, air-dried		**Magnesium+Glycerol**		**K-saturated, air-dried**		**K-saturated+Heat**	
d-spacing(Å)	*% Intensity*	*d-spacing(Å)*	*% Intensity*	*d-spacing(Å)*	*% Intensity*	*d-spacing(Å)*	*% Intensity*
14.47	100.0	18.45	100.0	12.68	100.0	13.88	100.0
8.52	6.8	14.47	38.7	7.24	98.7	10.10	85.9
7.33	26.4	9.44	14.3	7.03	67.9	8.36	28.1
7.12	24.7	9.03	13.9	4.71	28.2	7.23	57.6
4.75	10.9	8.50	8.3	3.62	24.4		
3.65	7.3	7.33	42.6	3.52	32.1		
3.56	11.7	7.12	29.1	3.13	15.4		
3.14	6.3	4.75	12.2				
		3.64	17.0				
		3.55	19.6				
JR3515CLAY: Depth 5-15 cm							
Mg-Saturated, air-dried		**Magnesium+Glycerol**		**K-saturated, air-dried**		**K-saturated+Heat**	
d-spacing(Å)	*% Intensity*	*d-spacing(Å)*	*% Intensity*	*d-spacing(Å)*	*% Intensity*	*d-spacing(Å)*	*% Intensity*
14.47	100.0	17.24	100.0	12.97	100.0	13.96	100.0
8.42	4.5	13.97	44.7	7.41	95.7	11.75	70.8
7.30	31.8	9.23	17.6	7.15	68.6	10.37	94.4
7.10	25.5	8.40	11.8	4.77	27.1	8.37	13.9
4.75	9.7	7.17	46.5	3.67	40.0	7.26	37.5
3.57	13.3	4.68	18.2	3.57	38.6		
3.13	9.1	3.62	19.4	3.15	28.6		
		3.52	22.9				
JR33045CLAY: Depth 30-45 cm							
Mg-Saturated, air-dried		**Magnesium+Glycerol**		**K-saturated, air-dried**		**K-saturated+Heat**	
d-spacing(Å)	*% Intensity*	*d-spacing(Å)*	*% Intensity*	*d-spacing(Å)*	*% Intensity*	*d-spacing(Å)*	*% Intensity*
14.47	100.0	18.69	100.0	12.68	100.0	13.93	62.7
8.42	4.4	14.76	28.7	7.37	84.3	10.49	100.0
7.30	20.7	9.54	10.7	7.15	53.9	8.37	19.0
7.10	18.2	9.15	10.7	4.79	15.7	7.23	11.1
4.75	6.9	8.60	6.1	3.66	30.3		
3.64	6.9	7.40	33.2	3.56	29.2		
3.56	7.4	7.17	25.6	3.15	31.5		
3.13	5.7	4.78	11.1				
		3.67	14.1				
		3.57	11.5				

*See Methods Section for details.

scattered (fig. 11C). These X-ray microprobe analyses provide a complimentary method for examining Cr geochemistry (including Cr(III) and Cr(VI)) in naturally occurring soil and rock solids; however, Cr(III) is the only detected valence state in serpentine soils and rocks at Jasper Ridge.

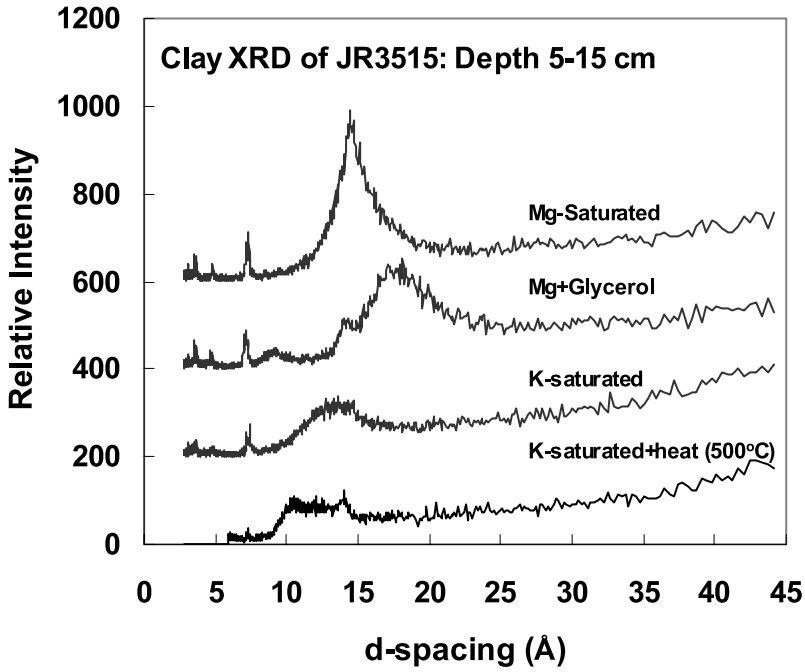

Fig. 9. XRD clay analyses of sample JR3515 (Site JR3, fig. 1B) demonstrate the influence of each treatment: Mg-saturated, Mg+glycerol, K-saturated, and K-saturated + heat (500°C). The d-spacings and percent intensities are also listed in table 7.

Sequential Extractions

Sequential extractions were completed on 1) Diablo clay (Inceptisol) from Site 1 (fig. 1B) at a depth of 10 centimeters, 2) serpentine soil (Mollisol) from Site 2 (fig. 1B) at a depth of 4 centimeters, and 3) commercial grade chromite (106 - 250 μm) and these results are listed in table 9. Chromium extracted from the exchangeable fraction is minimal (< 0.1 mg kg^{-1}) for all the samples (number 1 in table 9). Minor Cr concentrations are associated with the crystalline Fe-oxide fraction in the Diablo clay (1.9 Cr mg kg^{-1}) and serpentine soil (7.8 Cr mg kg^{-1}), whereas, chromite only released 0.5 Cr mg kg^{-1} (number 2 in table 9). Increased concentrations of Ni and Fe are present in the Fe-oxide fraction of the Diablo clay (161 Ni mg kg^{-1} and 447.4 Fe mg kg^{-1}) and serpentine soil (513.8 Ni mg kg^{-1} and 513.8 Fe mg kg^{-1}; tab. 9). Chromium extracted from the Diablo clay, serpentine soil, and chromite in the silicate fraction is 14, 31, and 1.4 Cr mg kg^{-1} respectively (number 3 in table 9). The sum of extracted Cr, Fe, Ni, and Mn concentrations (number 4 in table 9) is low with respect to total metals (number 5 in table 9). In fact, only 0.7, 1.2, and 0.0 percent of the total Cr was removed from the Diablo clay, serpentine soil, and chromite respectively (number 6 in table 9).

Chromite was extremely resistant to all the extractions and less than 0.01 percent of the total Cr was removed (table 9). Scanning electron microprobe (SEM) images of the chromite after each extraction are shown in figure 12. Chromium concentrations released from the chromite (table 9 and fig. 12A) increased with each sequential extraction experiment starting with the exchangeable fraction (fig. 12B), progressing into the crystalline Fe-oxide fraction (fig. 12C), and ending with the silicate fraction (fig. 12D). The surface of the chromite became smoother after each extraction and crystal imperfections in defect sites located along the edges and corners progressively

TABLE 8

X-ray diffraction d-spacings for common silicates from Whittig and Allardice (1986)

Diffraction Spacing (Å)	Mineral(s) Indicated
Mg-saturated, air-dried	
14-15	Smectite, vermiculite, chlorite
9.9-10.1	Mica (illite)
7.1-7.3	Serpentine
7.15	Kaolinite, chlorite
Mg-saturated, glycerol-solvated	
17.7-18.0	Smectite
14-15	Vermiculite, chlorite
9.9-10.1	Mica (illite)
7.1-7.3	Serpentine
7.15	Kaolinite, chlorite
K-saturated, air-dried	
14-15	Chlorite, vermiculite (with hydroxy interlayer)
12.4-12.8	Smectite
9.9-10.1	Mica, vermiculite (contracted)
7.1-7.3	Serpentine
7.15	Kaolinite, chlorite
K-saturated, heated (500°C)	
14	Chlorite
9.9-10.1	Mica, vermiculite (contracted), smectite (contracted)
7.1-7.3	Serpentine
7.15	Chlorite

decreased (fig. 12). Chromite does not appear to be an easily accessible source of Cr based on these extraction experiments.

DISCUSSION

Serpentinite at Jasper Ridge has undergone significant physical and chemical alteration since its formation and emplacement off the California continental margin. Jasper Ridge serpentinites are enriched with Cr, Co, Fe, Mg, Mn, and Ni compared to chert and sandstone located adjacent to the main serpentinite body (table 1 and fig. 1B). We infer that over the past 400,000 years, Cr-bearing minerals in the serpentinite have been weathering and accumulating in the soil. During this time, Cr concentrations in the soil have progressively increased relative to Cr-concentrations in the serpentinite protolith. This Cr enrichment is directly linked to specific weathering-resistant minerals identified in the soil.

Chromium in Serpentinites

Three minerals in the bedrock at Jasper Ridge contain appreciable concentrations of Cr: Cr-magnetite (8.2 - 10.3 Cr wt. %), chromite (~10.8 Cr wt. %), and CSM (~13.3 Cr wt. %). Cr-magnetite and CSM were derived from the alteration of primary igneous chromite. CSM or Cr-spinels with high concentrations of Si have been noted by (Burkhard, 1993) as a Cr-spinel containing a possible microscopic silicate phase. Our analyses support this result in which the microcrystalline silicate is probably Cr-chlorite due to its common occurrence with CSM (fig. 6). Definitive identification of this microcrystalline mixture was not possible due to size of the crystals relative to the spot

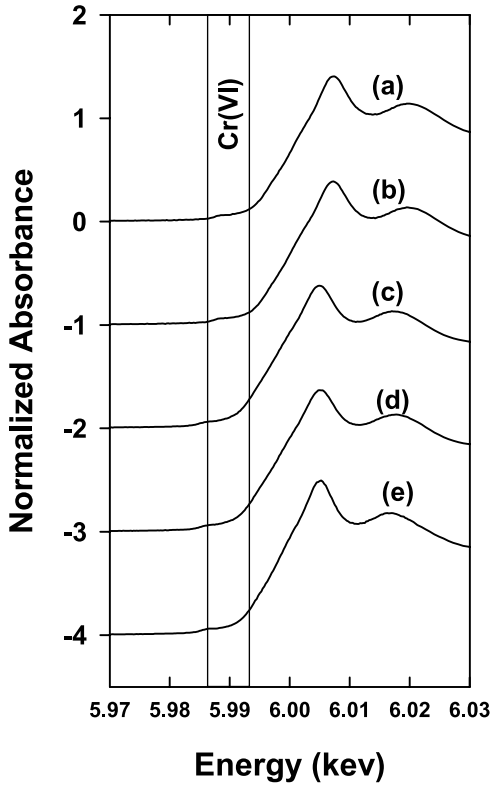

Fig. 10. Cr K XANES spectra for soils analyzed from Jasper Ridge serpentine soil at depths (a) 0–5 cm (b) 5–15 cm (c) 15–30 cm (d) 30–45 cm and (e) bedrock. The pre-edge area indicative of Cr(VI) peaks is shown on the right. Note that no peaks are present.

size of the electron microprobe. Chlorite and pyroxene contain minor concentrations of Cr (~1 wt. %) and these were the only identified Cr-containing silicates in the serpentinite. Minor concentrations of Cr observed in some chlorites are directly related to the metasomatic alteration of chromite and Cr-magnetite (fig. 6). The absence of other common metasomatically-derived Cr-bearing silicates such as fuchsite/mariposite and uvarovite probably records a lack of K^+ and Ca^{2+} in the alteration fluids. Overall, the chemical compositions of these protolith minerals (fig. 4) demonstrate only minor chemical variations, allowing comparative analysis with Cr-bearing soil minerals.

Chromium in Serpentine Soils

Cr-bearing soil minerals identified using the electron microprobe include chromite, Cr-magnetite, and CSM and these phases are chemically distinct from those in the bedrock (figs. 4 and 8). The highest concentration of Cr (41 wt. %) in the soil is in chromite with a composition approaching the $FeCr_2O_4$ end-member. This amount of Cr represents about an ~80 percent increase in the Cr concentration relative to bedrock chromite (see fig. 13). Cr-magnetite also demonstrates Cr enrichment (up to 20 Cr wt. %) with respect to magnetite identified in the bedrock (~10 Cr wt. %) (figs. 4 and 8). The textures of the soil Cr-bearing spinels exhibit sharp irregular edges possibly due to extensive weathering. CSM in the soil is similar to those found in the

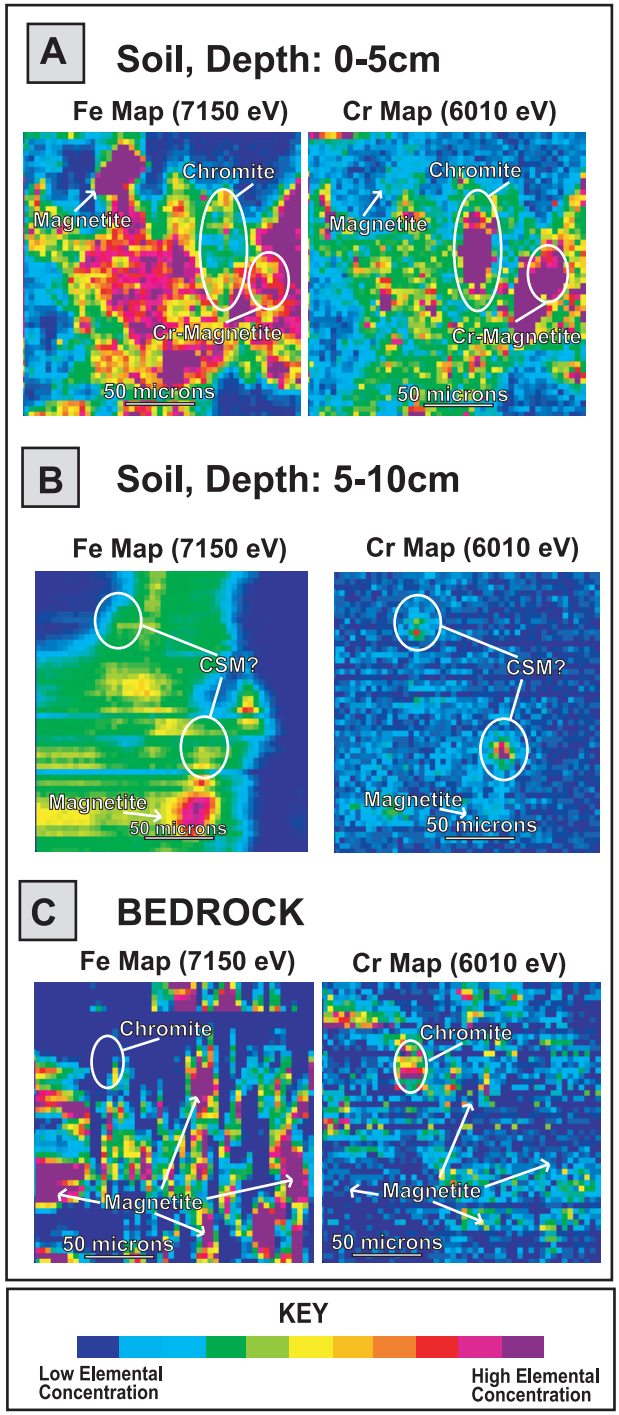

Fig. 11. X-ray microprobe elemental maps of Cr and Fe for (11A) serpentine soil at a depth of 0–5 cm, (11B) serpentine soil at a depth of 5–10 cm, and (11C) serpentinite bedrock at Jasper Ridge site JR3 (fig. 1B).

TABLE 9

Diablo clay, serpentine soil, and chromite sequential extractions

1. *Exchangeable Fraction (1mM $BaCl_2$)*			
	Diablo Clay	Serpentine Soil	Chromite
Element	mg kg^{-1}		
Cr	0	0	0.03
Fe	0.14	0.11	0.01
Ni	1.04	1.03	0.08
Mn	0	0	0

2. *Fe-Oxide Fraction (1M NH_2OH HCl in 25% (v/v) HOAc)*			
	Diablo Clay	Serpentine Soil	Chromite
Element	mg kg^{-1}		
Cr	1.9	7.8	0.5
Fe	447.4	513.8	3.8
Ni	161.0	150.6	0.1
Mn	23.1	43.0	0.0

3. *Silicate Fraction (10M HF)*			
	Diablo Clay	Serpentine Soil	Chromite
Element	mg kg^{-1}		
Cr	14.0	31.0	1.4
Fe	2,033.7	2,039.3	105.8
Ni	23.4	35.2	2.2
Mn	54.7	74.2	0.4

4. *Sum of 1, 2, & 3 (mg kg^{-1})*			
	Diablo Clay	Serpentine Soil	Chromite
Element	mg kg^{-1}		
Cr	15.9	38.8	1.9
Fe	2,481.2	2,553.2	109.6
Ni	185.4	186.8	2.5
Mn	77.8	117.2	0.4

5. *Total Cr, Fe, Ni, and Mn (Total Digestion)*			
	Diablo Clay	Serpentine Soil	Chromite
Element	mg kg^{-1}		
Cr	2,290	3,310	176,786.4
Fe	60,000	68,000	104,432.5
Ni	1,673	2,345	0.0
Mn	1,498	1,608	3,424.6

6. *Percent Extractable ((4/5)*100)*			
	Diablo Clay	Serpentine Soil	Chromite
Element	%		
Cr	0.7	1.2	0.0
Fe	4.1	3.8	0.1
Ni	11.1	8.0	0.0
Mn	5.2	7.3	0.0

*ICP-OES analyses

bedrock with Cr concentrations ranging from 11 to 14 Cr weight percent; however, Si concentrations in soil CSMs (8 to 14 wt. %) are noticeably less than those measured in the serpentinite (15 to 20 wt. %). The weathering of CSM might preferentially release Si relative to other elements in its structure. Cr-silicates (chlorite and pyroxenes) were not identified in the soil using the electron microprobe possibly due to complete weathering of these phases or they were too fine-grained for microprobe analyses; however, Cr-clinochlore was identified in the clay-size fraction using XRD. Elemental maps shown in figure 11 corroborate electron microprobe observations by revealing well-defined zones of Cr and Fe enrichment in both the soils and serpentinite. These areas of Cr and Fe enrichment are either chromite, Cr-magnetite, CSM, or magnetite. Overall, these maps reveal Cr is not homogeneously distributed in the soil confirming Cr is in specific mineral phases. Additionally, the observed abundance of chromite, Cr-magnetite, and CSM in the soils indicates that these minerals are probable sources for a majority of the Cr enrichment identified in the soils.

Soil Spinels

Soil chromite and Cr-magnetite appear to have undergone chemical alteration enriching the minerals with respect to Cr. In figure 13, compositions of bedrock chromite and end-member $FeCr_2O_4$ are shown together with tie-lines like those in figure 8 connecting both minerals. Reaction progress in figure 13 is based on the assumption that the serpentinite chromite (0 % reaction progress) is proceeding toward $FeCr_2O_4$ (100 % reaction progress) in the serpentine soil. Soil chromites from Jasper Ridge are also plotted in figure 13 where Cr concentrations are assumed to vary linearly between the bedrock chromite and chromite end-member defining the reaction progress of the mineral. These tie-lines correlate extremely well to the chemical composition of chromites identified in the soil. For example, chromite containing ~30 Cr weight percent will have ~15 Fe weight percent, ~13 Al weight percent, and ~5 Mg weight percent similar to soil chromite in figure 8. The retention of Cr in chromite shown in figure 13 has significant implications towards the availability and cycling of Cr in serpentine soils.

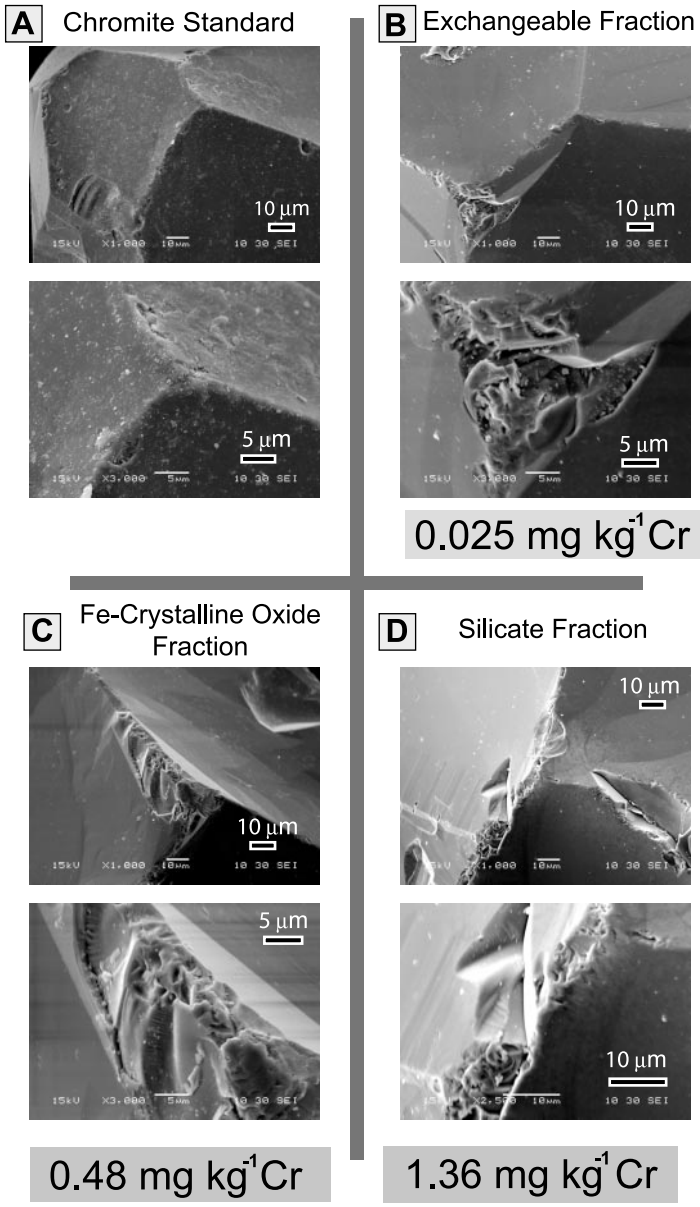

Fig. 12. SEM images of the chromite standard (A) after each sequential extraction treatment including the (B) exchangeable fraction (C) crystalline Fe-oxide fraction and (D) silicate fraction. The concentration of Cr removed by each treatment is shown beneath each set of images.

One possible mechanism for the chromite composition trends illustrated in figures 8 and 13 is incongruent dissolution where Cr is retained relative to other elements. Sequential extraction experiments (table 9) support this idea in which Fe is more easily released than Cr (109.6 Fe mg kg^{-1} to 1.9 Cr mg kg^{-1}) from chromite. Unfortunately, Mg and Al were not monitored during these extraction experiments; however, soil chromite microprobe analyses (fig. 13) show that Al and Mg have been

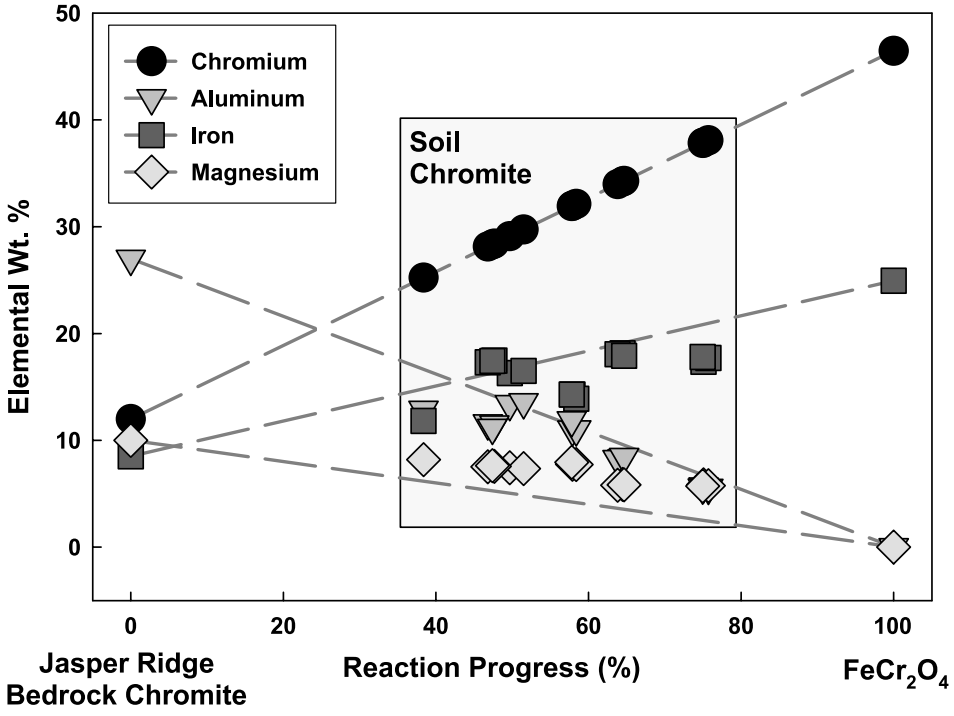

Fig. 13. Tie-lines connecting bedrock chromite and end-member $FeCr_2O_4$ and soil spinel analyses from figure 8 are shown on this single plot in order to demonstrate the incongruent dissolution of the soil spinels. Reaction progress is based on two assumptions: 1) the spinels are proceeding toward end-member $FeCr_2O_4$ and 2) Cr is conserved during spinel dissolution. For a sum of 100 weight percent, oxygen must be added to the sum of Cr, Al, Fe, and Mg weight percent.

preferentially released from the chromite structure compared to Fe and Cr. Additionally, the alterations of chromite in the serpentinite and the soils are analogous to one another. Chromite in the serpentinite retains a majority of its Cr compared to Mg and Al when altered to CSM by fluids at elevated pressures and temperatures (fig. 6 and table 2). Under ambient soil conditions, chromite once again retains Cr relative to Mg and Al, causing an apparent increase in Cr concentration. Chromium is not easily released from chromite whether under high pressures and temperatures or in the soil.

Crystal field stabilization energies (CFSE) and octahedral site preference energy parameters (OSPE) provide a potential means to explain the incongruent dissolution or Cr preservation in the Cr-spinels. CFSE is a measure of the net energy of stabilization gained by a metal ion's nonbonding d electrons as a result of complex formation. This measure also indirectly describes the energy required to remove an ion from a crystal structure. The octahedral CFSE for Cr(III) is –224.7 kJ $mole^{-1}$ and the OSPE (the difference between the tetrahedral and octahedral CFSE) is –157.8 kJ $mole^{-1}$ (Dunitz and Orgel, 1957; McClure, 1957). These values for Cr(III) are the most negative of those for any transition element, indicating that the incorporation of Cr(III) in an oxide has the potential to increase the crystal's stability compared to an analogous crystal lacking Cr(III). Chromium(III) would be among the last ions to be removed from the spinel structure compared to other transition elements, such as $Fe^{3+}$and Mn^{2+}.

TABLE 10

Chromite masses required for determined Cr concentrations (mg kg^{-1}) in 1 kg of sample

Cr Concentration (mg kg^{-1})	Chromite $FeCr_2O_4$	
	Grams	*Sample %*
500	1.1	0.11
1,000	2.2	0.22
2,000	4.3	0.43
5,000	10.8	1.08

Soil Chemistry Related to Chromium Availability

In table 5, the chemical properties of the soil at Site JR3 do not appear to be a factor when evaluating Cr in the soil. The pH of the soil did not vary considerably with depth. Additionally, Cr-mineral dissolution is at a near minimum around pH 7. Organic matter within the soil was elevated despite the low plant productivity of the serpentine soil. The decay of organic matter produces organic acids that could promote the dissolution of Cr-bearing minerals; however, Cr concentrations near the surface (where organic matter was the greatest) are not significantly greater or less than those deeper in the soil profile. The relative concentrations of ammonium acetate extractable Ca, K, Mg, and Na are characteristic of serpentine soils and did not provide any new insight. Finally, Cr(III) was the only identifiable valence state of Cr based on X-ray absorption spectroscopy (fig. 10) which is what should be expected based on the Cr-bearing minerals and the pH of the soil.

Extraction experiments summarized in table 9 demonstrate that ~99 percent of the Cr in a serpentine soil is retained in highly resistant phases at Jasper Ridge. The chromite standard used in these experiments contributed negligible concentrations of Cr ($<$ 2 mg kg^{-1} total) for all of the sequential extraction experiments supporting earlier evidence that Cr-spinels are retaining Cr and are potentially responsible for a majority of the total Cr enrichment in the serpentine soil. At Jasper Ridge, Cr extracted from the serpentine soil (31 mg kg^{-1}) is likely the result of the Cr-silicates compared to the Cr-spinels. Low Cr-containing minerals (possibly chlorite, enstatite, augite, and clay minerals) appear to be the most probable source of Cr to soil solutions and vegetation of the serpentine soil. Approximately 30 percent of the serpentine soil is composed of clay-sized minerals and this size-fraction has ~1,000 Cr mg kg^{-1}. The mineral responsible for Cr enrichment in the clay-size fraction is more than likely Cr-chlorite or possibly smectite, identified using XRD.

The enrichment pattern of Cr in serpentine soils (fig. 7) can be explained by the abundance of Cr-spinels. Small grains of chromite, Cr-magnetite, and even CSM in the soil have the potential to appreciably impact Cr concentrations. Table 10 demonstrates the chromite masses required to change the Cr concentration in a 1-kilogram sample of soil. The highest Cr concentration at Jasper Ridge was identified at Site 3 with a measured value of 4,760 mg kg^{-1} which means only ~1 percent of the soil sample (table 10) needs to contain chromite. Additionally, a minimal amount ($<$ 0.11 % of the sample as shown in table 10) of chromite is necessary to change the concentration by 500 mg kg^{-1}, which could easily cause the sharp Cr increases and decreases noted in figure 7. This small amount of chromite agrees with our observations of chromite abundance in the serpentine soils. Additionally, most of the chromite grains identified in the bedrock are between 2 and 0.02 millimeters, which correspond directly to the elevated Cr concentrations ($>$ 10,000 mg kg^{-1}) in the sand-size fraction of the serpentine soil (table 6). Even the ~15,000 Cr mg kg^{-1} values in soils measured by

Hotz (1964) in figure 2 only require ~2 percent of the sample to contain chromite. A few chromite grains possess the ability to significantly impact measured Cr concentrations in soil samples.

Chromium and Nickel in Serpentine Soils

Chromium and Ni have often been correlated with one another due to their common enrichment in serpentine soils (Hotz, 1964; Rabenhorst and others, 1982; Schwertmann and Latham, 1986; Schreier and others, 1987; Brooks, 1987; Alexander and others, 1989; Kaupenjohann and Wilcke, 1995). A majority of the Ni in the Jasper Ridge serpentine soil originated from olivine (fig. 5C and 5D; table 3). Chemical alteration of olivine during serpentinization resulted in the mineral serpentine (Coleman and Jove, 1992) which contains minor concentrations of Ni (< 0.37 NiO wt. %). Continued alteration under highly reducing conditions, coupled with the incompatibility of Ni in the serpentine structure, resulted in the formation of Ni-Fe alloy (fig. 5C). This type of alteration is observed in many of the rocks at Jasper Ridge where the Ni-Fe alloy grains are ~10 μm in size. Olivine in the rocks and soil is less resistant to weathering compared to chromite; therefore, Ni is possibly more available to bacteria and vegetation in serpentine soils than Cr. Sequential extractions (table 9) support these observations. Although Cr and Ni are enriched in serpentine soils, the availability and behavior of these two elements are significantly different.

CONCLUDING REMARKS

Chromium is predominantly present in primary chromite, Cr-magnetite, and a chromite-silicate mixture (CSM) in both the bedrock and soil despite weathering over geologic time. Sharp variations in soil Cr concentrations with respect to depth are caused by the presence or absence of chromite, Cr-magnetite, and/or CSM. Chromium-spinels in the soil have undergone incongruent dissolution possibly conserving Cr(III) with respect to Al^{3+} and Mg^{2+}. Chromite is highly resistant to weathering and it is more than likely not contributing bioavailable Cr. Although Cr-spinels account for most of the Cr, Cr-silicates in the protolith (chlorite, enstatite, and augite) and soil (chlorite, montmorillonite, and vermiculite) contain the most accessible Cr. Chlorite and smectite are the most likely sources of Cr from these silicate minerals. Finally, Cr(VI) was not detected in any of the soil and rock samples.

ACKNOWLEDGMENTS

We thank Jasper Ridge Biological Preserve for allowing us the opportunity to examine the serpentine soils. Funding from the JRBP Mellon Grant, Stanford Shell Foundation, Stanford McGee Fund, NSF Grant EAR-9902859 (DKB), GSA Graduate Student Research Grants, and the Office of Teaching and Learning (SF) at Stanford University is gratefully acknowledged. We appreciate the technical support from the staff of the Stanford Synchrotron Radiation Laboratory, from Bob Jones for assistance in microprobe analyses of the serpentinites and serpentine soils, and from Ben Bostick, Travis Horton, and Theresa Barber for field and lab assistance. This manuscript was much improved by three anonymous reviewers.

REFERENCES

Alexander, E. B., Adamson, C., Zinke, P. J., and Graham, R. C., 1989, Soils and conifer forest productivity on serpentinized peridotite of the Trinity Ophiolite, California: Soil Science, v. 148, p. 412–423.

Ball, J. W., and Nordstrom, D. K., 1998, Critical-evaluation and selection of standard state thermodynamic properties for chromium metal and its aqueous ions; hydrolysis species; oxides; and hydroxides: Journal of Chemical and Engineering Data, v. 43, p. 895–918.

Becquer, T., Quantin, C., Sicot, M., and Boudot, J. P., 2003, Chromium availability in ultramafic soils from New Caledonia: Science of the Total Environment, v. 301, p. 251–261.

Brady, N. C., and Weil, R. R., 1999, The Nature and Properties of Soils: Upper Saddle River, Prentice-Hall, 881 p.
Brooks, R. R., 1987, Serpentine and Its Vegetation: Ecology, Phytogeography & Physiology Series, v. 1: Portland, Dioscorides Press, 454 p.
Burgmann, R., Arrowsmith, R., Dumitru, T., and McLaughlin, R. J., 1994, Rise and fall of the southern Santa Cruz Mountains, California, from fission tracks, geomorphology, and geology: Journal of Geophysical Research, v. 99, p. 20181–20202.
Burkhard, D. J. M., 1993, Accessory chromium spinels: Their coexistence and alteration in serpentinites: Geochimica et Cosmochimica Acta, v. 57, p. 1297–1306.
Challis, A., Grapes, R., and Palmer, K., 1995, Chromian muscovite, uvarovite, and zincian chromite: Products of regional metasomatism in northwest Nelson, New Zealand: Canadian Mineralogist, v. 33, p. 1263–1284.
Charlet, L., and Manceau, A., 1992, X-ray absorption spectroscopic study of the sorption of Cr(III) at the oxide water interface 2. Adsorption, coprecipitation, and surface precipitation on hydrous ferric-oxide: Journal of Colloid and Interface Science, v. 148, p. 443–458.
Chen, P., and Lee, C. W., 1974, Fuchsite in gold-bearing rock from Laochi, Hualien: Acta Geologica Taiwanica, v. 17, p. 7–11.
Chester, R., and Hughes, M. J., 1967, A chemical technique for the separation of ferro-manganese minerals, carbonate minerals, and adsorbed trace elements for pelagic sediments: Chemical Geology, v. 2, p. 249–262.
Christofides, G., Thimiatis, G., Koroneos, A., Sklavounos, S., and Eleftheriadis, G., 1994, Mineralogy and chemistry of Cr-chlorites associated with chromites from Vavdos and Vasilika Ophiolite Complexes (Chalkidiki, Macedonia, N. Greece): Chemie der Erde, v. 54, p. 151–166.
Cohen, M. D., Kargacin, B., Klein, C. B., and Costa, A. M., 1993, Mechanisms of chromium carcinogenicity and toxicity: Critical Reviews in Toxicology, v. 23, p. 255–281.
Cole, M. M., 1992, The vegetation over mafic and ultramafic rocks in the Transvaal Lowveld, South Africa, *in* Roberts, B. A., and Proctor, J., editors, The ecology of areas with serpentinized rocks. A world view: Netherlands, Kluwer Academic Publishers, p. 333–342.
Coleman, R. G., and Jove, C., 1992, Geological origin of serpentinites, *in* Baker, A. J. M., Proctor, J., and Reeves, R. D., editors, The Vegetation of Ultramafic (Serpentine) Soils: Andover, Intercept, p. 1–17.
Cooper, A. F., 1980, Retrograde alteration of chromian kyanite in metachert and amphibolite whiteschist from the Southern Alps, New Zealand, with implications for uplift on the Alpine Fault: Contributions to Mineralogy and Petrology, v. 75, p. 153–164,
Daugherty, M. L., 1992, Toxicity Summary for Chromium, Chemical Hazard Evaluation and Communication Group: Oak Ridge, Oak Ridge National Laboratory, p. 26.
Deer, W. A., Howie, R. A., and Zussman, J., 1996, An Introduction to the Rock-Forming Minerals: Essex, Longman, 696 p.
Dunitz, J. D., and Orgel, L. E., 1957, Electronic properties of transition-metal oxides. II. Cation distribution amongst octahedral and tetrahedral sites: Physics and Chemistry of Solids, v. 3, p. 318–323.
Ernst, W. G., 1971, Do mineral parageneses reflect unusually high pressure conditions of Franciscan metamorphism?: American Journal of Science, v. 271, p. 81–108.
Fendorf, S. E., 1995, Surface reactions of chromium in soils and waters: Geoderma, v. 67, p. 55–71.
Gasser, U. G., and Dahlgren, R. A., 1994, Solid-phase speciation and surface association of metals in serpentinitic soils: Soil Science, v. 158, p. 409–420.
Gee, G. W., and Bauder, J. W., 1986, Particle-size Analysis, *in* Page, A. L., editor, Methods of soil analysis, Part 1, Physical and mineralogical methods: Madison, American Society of Agronomy, p. 383–411.
Gerth, J., 1990, Unit-cell dimensions of pure and trace metal-associated goethites: Geochimica et Cosmochimica Acta, v. 54, p. 363–371.
Gough, L. P., Meadows, G. R., Jackson, L. L., and Dudka, S., 1989, Biogeochemistry of a highly serpentinized, chromite-rich ultramafic area, Tehama County, California: U. S. Geological Survey Bulletin 1901, p. 1–24.
Green, J., 1972, Elements: planetary abundances and distribution, *in* Fairbridge, R. W., editor, Encyclopedia of Geochemistry and Environmental Sciences IVA: New York, Van Nostrand Reinholt, p. 268–300.
Hoffman, M. A., and Walker, D., 1978, Textural and chemical variations of olivine and chrome spinel in the East Dover ultramafic bodies, south-central Vermont: Geological Society of America Bulletin, v. 89, p. 699–710.
Hostetler, P. B., Coleman, R. G., and Mumpton, F. A., 1966, Brucite in alpine serpentinites: American Mineralogist, v. 51, p. 75–80.
Hotz, P. E., 1964, Nickeliferous laterites in southwestern Oregon and northwestern California: Economic Geology, v. 59, p. 355–396.
Ilton, E. S., and Veblen, D. R., 1994, Chromium sorption by phlogopite and biotite in acidic solutions at 25 C: Insights from X-ray photoelectron spectroscopy and electron microscopy: Geochimica et Cosmochimica Acta, v. 58, p. 2777–2788.
Ilton, E. S., Moses, C. O., and Veblen, D. R., 2000, Using X-ray photoelectron spectroscopy to discriminate among different sorption sites of micas: With implications for heterogeneous reduction of chromate at the mica-fluid interface: Geochimica et Cosmochimica Acta, v. 64, p. 1437–1450.
James, B. R., Petura, J. C., Vitale, R. J., and Mussoline, G. R., 1997, Oxidation-reduction chemistry of chromium: Relevance to the regulation and remediation of chromate-contaminated soils, *in* Proctor, D. M., Finley, B. L., Harris, M. A., Paustenbach, D. J., and Rabbe, D., editors, Chromium in Soil: Perspectives in Chemistry, Health, and Environmental Regulation: Boca Raton, Lewis Publishers, p. 561–568.

Kashiwagi, J. H., 1985, Soil survey of Marin County, California: Washington D. C., U. S. Department of Agriculture, Soil Conservation, 229 p.
Kaupenjohann, M., and Wilcke, W., 1995, Heavy metal release from a serpentine soil using a pH-stat technique: Soil Science Society of America Journal, v. 59, p. 1027–1031.
Kerrich, R., Fyfe, W. S., Barnett, R. L., Blair, B. B., and Willmore, L. M., 1987, Corundum, Cr-muscovite rocks at O'Briens, Zimbabwe: The conjunction of hydrothermal desilicification and LIL-element enrichment-geochemical and isotopic evidence: Contributions to Mineralogy and Petrology, v. 95, p. 481–498.
Kruckeberg, A. R., 1992, Plant life of western North American ultramafics, *in* Roberts, B. A., and Proctor, J., editors, The Ecology of Areas with Serpentinized Rocks. A World View: Netherlands, Kluwer Academic Publishers, p. 31–73.
Kunze, G. W., and Dixon, J. B., 1986, Pretreatment for mineralogical analysis, *in* Klute, A., editor, Methods of Soil Analysis, Part 1. Physical and Mineralogical Methods: Madison, American Society of Agronomy-Soil Science Society of America, p. 91–99.
Leo, G. W., Rose, H. J., and Warr, J. J., 1965, Chromian muscovite from the Serra de Jacobina, Bahia, Brazil: The American Mineralogist, v. 50, p. 392–402.
Li, G. C., and Fendorf, S. E., 2000, Organic-ligand promoted chromium mobilization in soil: Minneapolis, SSSA Annual Meeting.
Malpas, J., 1992, Serpentine and the geology of serpentinized rocks, *in* Roberts, B. A., and Proctor, J., editors, The Ecology of Areas with Serpentinized Rocks. A World View: Netherlands, Kluwer Academic Publishers, p. 7–30.
Mathiesen, L., ms, 1999, A petrographic study of Ba-Cr-muscovite from Isua, SW-Greenland: Masters of Science Thesis, University of Copenhagen, Denmark.
Max, M. D., Treloar, P. J., Winchester, J. A., and Oppenheim, M. J., 1983, Cr mica from the Precambrian Erris Complex, NW Mayo, Ireland: Mineralogical Magazine, v. 47, p. 359–364.
McBride, M. B., 1994, Environmental Chemistry of Soils: New York, Oxford University Press, 406 p.
McClure, D. S., 1957, The distribution of transition metal cations in spinels: Physics and Chemistry of Solids, v. 3, p. 311–317.
Mebius, L. J., 1960, A rapid method for the determination of organic carbon in soil: Analytica Chimica Acta, v. 22, p. 120–124.
Page, B. M., and Tabor, T. L., 1967, Chaotic structure and decollement in Cenozoic rocks near Stanford University, California: Geological Society of America Bulletin, v. 78, p. 1–12.
Pan, U., and Fleet, M. E., 1991, Barian feldspar and barian-chromian muscovite from the Hemlo Area, Ontario: The Canadian Mineralogist, v. 29, p. 481–498.
Peterson, M. L., 1996, Chromium (VI) Reduction by Magnetite: Spectroscopic Evidence of Sorption, Precipitation, and Heterogeneous Oxidation-Reduction Reactions, Environmental & Geological Sciences: Stanford, Stanford University, p. 115.
Phillips, T. L., Loveless, J. K., and Bailey, S. W., 1980, Cr^{3+} coordination in chlorites: a structural study of ten chromian chlorites: American Mineralogist, v. 65, p. 112–122.
Proctor, J., 1992, The vegetation over ultramafic rocks in the tropical far east, *in* Roberts, B. A., and Proctor, J., editors, The Ecology of Areas with Serpentized Rocks. A World View: Netherlands, Kluwer Academic Publishers, p. 249–270.
Raase, P., Raith, M., Ackermand, D., Viswanatha, M. N., and Lal, R. K., 1983, Mineralogy of chromiferous quartzites from South India: Journal Geological Society of India, v. 24, p. 502–521.
Rabenhorst, M. C., Foss, J. E., and Fanning, D. S., 1982, Genesis of Maryland soils formed from serpentinite: Soil Science Society of America Journal, v. 46, p. 607–616.
Roberts, B. A., 1992, Ecology of serpentinized areas, Newfoundland, Canada, *in* Roberts, B. A., and Proctor, J., editors, The Ecology of Areas with Serpentinized Rocks. A World View: Netherlands, Kluwer Academic Publishers, p. 75–113.
Robinson, W. O., Edgington, G., and Byers, H. G., 1935, Chemical studies of infertile soils derived from rocks high in magnesium and generally high in chromium and nickel: U.S. Department of Agriculture Technical Bulletin, v. 471, p. 1–28.
Sack, R. O., and Ghiorso, M. S., 1991, Chromian spinels as petrogenetic indicators: Thermodynamics and petrological applications: American Mineralogist, v. 76, p. 827–847.
Sanchez-Vizcaino, V. L., Franz, G., and Gomez-Pugnaire, M. T., 1995, The behavior of Cr during metamorphism of carbonate rocks from the Nevado-Filabridge Complex, Betic Cordilleras, Spain: The Canadian Mineralogist, v. 33, p. 85–104.
Schreier, H., Omueti, J. A., and Lavkulich, L. M., 1987, Weathering processes of asbestos-rich serpentinitic sediments: Soil Science Society of America Journal, v. 51, p. 993–999.
Schreyer, W., Werding, G., and Abraham, K., 1981, Corundum-fuchsite rocks in greenstone belts of Southern-Africa: Petrology, geochemistry and possible origin: Journal of Petrology, v. 22, p. 191–231.
Schwertmann, U., and Latham, M., 1986, Properties of iron oxides in some New Caledonian Oxisols: Geoderma, v. 39, p. 105–123.
Schwertmann, U., Gasser, U., and Sticher, H., 1989, Chromium-for-iron substitution in synthetic goethites: Geochimica et Cosmochimica Acta, v. 53, p. 1293–1297.
Spangenberg, K., 1943, Die Chromitlagerstatte von Tampadel am Zobten: Zeitschrift fur Praktische Geologie, v. 5, p. 13–25.
Sweeny, R. A., 1989, Generic combustion method for determination of crude protein in feeds: Collaborative study: Journal of the Association of Official Analytical Chemists, v. 72, p. 770–774.
Treloar, P. J., 1987, The Cr-minerals of Outokumpu—Their chemistry and significance: Journal of Petrology, v. 28, p. 867–886.
Turitzin, S. N., 1991, Nutrient limitations to plant growth in California serpentine grassland: American Midland Naturalist, v. 107, p. 95–99.

Vaniman, D., 2001, Clay mineral and zeolite separation: Los Alamos, Los Alamos National Laboratory, p. 8.
Von Knorring, O., Condliffe, E., and Tong, Y. L., 1986, Some mineralogical and geochemical aspects of chromium-bearing skarn minerals from Northern Karella, Finland: Bulletin Geological Society Finland, v. 58, p. 277–292.
Walker, R. B., 1954, Factors affecting plant growth on serpentine soils, *in* Whittaker, R. H., editor, The Ecology of Serpentine Soils: A Symposium. Ecology, p. 258–266.
Whitmore, D. R. E., Berry, L. G., and Hawley, J. E., 1946, Chrome micas: American Mineralogist, v. 31, p. 1–21.
Whittig, L. D., and Allardice, W. R., 1986, X-ray diffraction techniques, Methods of Soil Analysis, Part 1. Physical and Mineralogical Methods: Madison, American Society of Agronomy-Soil Science Society of America, p. 331–362.